

Galactic chemical evolution of heavy elements: from Barium to Europium

Claudia Travaglio¹

1. Dipartimento di Astronomia e Scienza dello Spazio, Largo E. Fermi 5, I-50125 Firenze,
Italy

Daniele Galli²

2. Osservatorio Astrofisico di Arcetri, Largo E. Fermi 5, I-50125 Firenze, Italy

Roberto Gallino³

3. Dipartimento di Fisica Generale, Università di Torino, Via P.Giuria 1, I-10125 Torino,
Italy

Maurizio Busso⁴

4. Osservatorio Astronomico di Torino, Strada Osservatorio 20, I-10025 Torino, Italy

Federico Ferrini⁵

5. Dipartimento di Fisica, Sezione di Astronomia, Università di Pisa, Piazza Torricelli 2,
I-56100 Pisa, Italy

Oscar Straniero⁶

6. Osservatorio Astronomico di Collurania, I-64100 Teramo, Italy

Received _____; accepted _____

ABSTRACT

We follow the chemical evolution of the Galaxy for elements from Ba to Eu, using an evolutionary model suitable to reproduce a large set of Galactic (local and non local) and extragalactic constraints. Input stellar yields for neutron-rich nuclei have been separated into their s -process and r -process components. The production of s -process elements in thermally pulsing asymptotic giant branch stars of low mass proceeds from the combined operation of two neutron sources: the dominant reaction $^{13}\text{C}(\alpha,n)^{16}\text{O}$, which releases neutrons in radiative conditions during the interpulse phase, and the reaction $^{22}\text{Ne}(\alpha,n)^{25}\text{Mg}$, marginally activated during thermal instabilities. The resulting s -process distribution is strongly dependent on the stellar metallicity. For the *standard* model discussed in this paper, it shows a sharp production of the Ba-peak elements around $Z \simeq Z_{\odot}/4$. Concerning the r -process yields, we assume that the production of r -nuclei is a primary process occurring in stars near the lowest mass limit for Type II supernova progenitors. The r -contribution to each nucleus is computed as the difference between its solar abundance and its s -contribution given by the Galactic chemical evolution model at the epoch of the solar system formation. We compare our results with spectroscopic abundances of elements from Ba to Eu at various metallicities (mainly from F and G stars) showing that the observed trends can be understood in the light of the present knowledge of neutron capture nucleosynthesis. Finally, we discuss a number of emerging features that deserve further scrutiny.

Subject headings: nucleosynthesis - stars: abundances, AGB and post-AGB - Galaxy: evolution, abundances

1. Introduction

A quantitative understanding of the Galactic evolution of nuclei heavier than iron has been so far a challenging problem. Although some of the basic tools of this task have been presented several years ago, both from an observational (Spite & Spite 1978, 1979; Sneden & Parthasarathy 1983; Gilroy et al. 1988) and a theoretical point of view (Truran 1981), only recently the observational data have grown sufficiently in number and precision to allow a direct comparison with theoretical predictions (see McWilliam 1995 for a review). In order to reconstruct the evolutionary history of neutron-rich elements in the Galaxy one has to disentangle the s - and r -contributions of all their isotopes and follow their abundance as a function of Galactic age. The results must then be compared with the available spectroscopic observations of stars at different metallicities, both in the Galactic halo and disk, mainly from F and G dwarfs and giants whose surface abundances reflect the composition of the gas from which they formed (Gratton & Sneden 1994; Edvardsson et al. 1993).

Already in the seminal work by Burbidge et al. (1957), the synthesis of neutron-rich nuclei was attributed to two different mechanisms. The first (the s -process) is characterized by *slow* neutron captures and occurs mainly during hydrostatic He-burning phases of stellar evolution. Here *slow* means that most unstable nuclei encountered along the neutron capture path have time to decay before capturing another neutron. The second mechanism (the r -process) is due to the more *rapid* neutron captures and is generally associated with explosive conditions in supernovae (hereafter SNe). For a comprehensive review on the astrophysical sites of neutron capture nucleosynthesis, see Wheeler, Sneden, & Truran (1989).

The current understanding of the s -process is supported by many observational and theoretical works (summarized in Sect. 2), indicating that the heavier s -nuclei, from Sr to Pb, belonging to the so-called *main* component (Clayton & Ward 1974; Käppeler et al. 1982), are synthesized during the thermally pulsing asymptotic giant branch (TP-AGB) phase of

low-mass stars, mainly in the mass range $\sim 1\text{--}4 M_{\odot}$ (see e.g. Gallino, Busso, & Lugaro 1997; Busso, Gallino, & Wasserburg 1999, hereafter BGW). A different site for the production of s -process nuclei is required to account for the *weak* component, i.e. for s -nuclei below the Sr-peak. This site was identified in the advanced evolutionary phases of massive stars (Lamb et al. 1977; Prantzos et al. 1990; Raiteri et al. 1993).

As for the r -process, the actual astrophysical environment is still a matter of debate (Woosley et al. 1994; Wheeler, Cowan, & Hillebrandt 1998). It has been recently shown that at least two different supernova sources are required for the synthesis of the r -nuclei below or beyond the neutron magic number $N = 82$ (Wasserburg, Busso, & Gallino 1996; see also Sneden et al. 1998). For the elements considered here, we make the simplifying hypothesis that their r -contributions in the solar system can be considered of primary origin (i.e. with yields independent of the initial stellar metallicity). Hence, after the s -contributions at the epoch of the solar formation have been estimated with the use of a reliable model for the chemical evolution of the Galaxy, the r -process abundance fractions can be derived by subtracting the s -fractions from the solar abundances.

The study of the Galactic evolution of elements produced by s - and r -processes was addressed in previous investigations only at a semi-quantitative level. For example, Andreani, Vangioni-Flam, & Audouze (1988), and, more recently, Pagel & Tautvaišienė (1997) have assumed *ad hoc* stellar yields and time delays for representative s and r elements in order to fit the observational data. With a different approach, Mathews, Bazan, & Cowan (1992), following a preliminary analysis by Clayton (1988), examined the effects introduced by the primary nature of the ^{13}C neutron source on the s -process yields, and inferred that for metallicities $Z > 10^{-3}Z_{\odot}$ the neutron exposure $\tau \equiv \int n_n v_T dt$ (where n_n is the neutron density and v_T the thermal velocity) roughly scales as Z^{-1} . Under the crude assumption that the production (in mass fraction) of a given s -isotope depends on the product of the

neutron exposure times the abundance of iron group seeds, Mathews et al. (1992) estimated the stellar s yields by simply scaling the solar s -abundances with metallicity. Today the work of Mathews et al. (1992) needs to be revised, as quantitative yields are now available from detailed nucleosynthesis calculations based on TP-AGB models for different masses and metallicities, with updated reaction networks and neutron capture cross sections. In addition, as anticipated by Truran (1981), at low metallicities the r -process contribution to the various elements becomes dominant.

In this paper, we concentrate on elements from Ba to Eu, not only because they belong to a major abundance peak, but also because they contain species of very different origin, ranging from almost pure r -process production, as is the case for Eu, to a dominant s -process origin, as is the case for Ba. The paper is organized as follows: in Sect. 2 we analyze the neutron capture process in AGB stars; in Sect. 3 we describe the adopted model for the chemical evolution of the Galaxy and the updates introduced in the present work; in Sect. 4 we show the model results for the elements considered (Ba, La, Ce, Pr, Nd, Sm, and Eu) and for their isotopes; finally, in Sect. 5 we summarize the main conclusions and point out a few aspects deserving further analysis.

2. The production of s -process nuclei in Asymptotic Giant Branch stars

2.1. Previous work

The first quantitative model for the production of s -process nuclei with $A > 85$ was presented by Truran & Iben (1977) and by Iben & Truran (1978). It was based on the activation of the $^{22}\text{Ne}(\alpha,n)^{25}\text{Mg}$ neutron source in TP-AGB stars of intermediate mass ($5 \lesssim M/M_{\odot} \lesssim 8$). However, subsequent reanalyses showed that the attempts to reproduce the solar main component through the $^{22}\text{Ne}(\alpha,n)^{25}\text{Mg}$ neutron source suffer from major nu-

clear problems (Despain 1980; Howard et al. 1986; Mathews et al. 1986; Busso et al. 1988). On the other hand, observations revealed that the luminosities of MS, S and C (N type) stars are generally much lower than predicted by the above models, thus pointing out that the dominant contributors to the synthesis of carbon and *s*-process elements are AGB stars of lower mass (see e.g. Clegg, Lambert, & Bell 1979; Blanco, McCarthy, & Blanco 1980; Smith & Lambert 1986; Lambert et al. 1991). In low-mass AGB stars the maximum temperature reached during thermal instabilities in the He shell is too low ($T_{\max} \simeq 3 \times 10^8$ K) for ^{22}Ne to be significantly consumed. Consequently, neutron captures must be driven by the alternative $^{13}\text{C}(\alpha, n)^{16}\text{O}$ reaction (Cameron 1954), which can easily be activated at much lower temperatures (for the rate of this reaction see Caughlan & Fowler 1988 and Denker et al. 1995).

The amount of ^{13}C left in the He intershell from previous H burning is by far too low to be of any relevance in the neutron production. A challenging problem is therefore to explain how a sufficient amount of ^{13}C can be built locally. The common hypothesis is that some protons can penetrate below the formal convective border of the envelope into the top layers of the He intershell. At H re-ignition, these protons are captured by the abundant ^{12}C left by partial He burning in the previous convective pulse, giving rise to a tiny layer enriched in ^{13}C (the so-called ^{13}C pocket). The first mechanism considered in order to generate a ^{13}C pocket was the semi-convective mixing of H into the ^{12}C -rich and He-rich intershell, driven by increased carbon opacity in the cool expanding envelope after the quenching of a thermal pulse (Iben & Renzini 1982a,b). This process was shown to be relevant for Population II stars (Hollowell & Iben 1988, 1989). Once formed, the ^{13}C pocket was assumed to be engulfed by the next convective pulse releasing neutrons. The resulting neutron density, originally estimated to be very high ($\geq 10^{11}$ n/cm³, see Malaney 1986) was subsequently shown to be of the order of $(5\text{--}10)\times 10^8$ n/cm³ (Käppeler et al 1990; Gallino, Raiteri, & Busso 1993). However, semiconvection was found to become inefficient in Galactic disk stars (Iben 1983),

and no obvious alternative from simple diffusive mixing was found to work (Iben 1982).

The penetration of the convective envelope into the partially He-burnt zone after each pulse (the so-called *third dredge-up*) leaves a sharp H/C discontinuity between the H-rich envelope and the ^{12}C -rich and He-rich intershell, which is likely to be smoothed by some sort of mixing at the interface, by chemical diffusion, semiconvection, or rotational shear (Langer et al. 1999). To address this point, a rather sophisticated treatment of the hydrodynamic behavior at the H/He boundary would be required. First attempts with a diffusive approach (Herwig et al. 1997), or with a fully hydrodynamical formulation (Singh, Roxburgh, & Chan 1998) have been recently presented and do show formation of a ^{13}C reservoir. Indeed, penetration of protons at the top of the ^{12}C -rich intershell appears to be plausible, but the mass involved and the resulting H profile have still to be treated as relatively free parameters. A dedicated effort on hydrodynamical grounds constitutes a major challenge for AGB calculations and *s*-process nucleosynthesis studies.

2.2. *s*-process yields from AGB stars: FRANEC results

A more indirect approach is to consider different choices for the mass and profiles of the ^{13}C pocket, and to estimate their effects on the nucleosynthesis results for AGB models of various metallicities. The TP-AGB models by Straniero et al. (1995, 1997) showed that any amount of ^{13}C produced by a proton penetration below the convective envelope border burns radiatively in the interpulse period, at a relatively low temperature ($T \gtrsim 0.9 \times 10^8$ K) and neutron density ($n_n \lesssim 10^7$ n/cm³), giving rise to a tiny layer extremely enriched in *s*-process isotopes that will be engulfed by the next convective instability. The resulting pattern of AGB nucleosynthesis, and its dependence on the initial metallicity of the star, have been recently discussed by Gallino et al. (1999). The changes introduced by these recent studies are important: not only the neutron density is lower by a factor of ~ 20 than in previous

estimates, but the distribution of neutron exposures can no longer be approximated by an exponential distribution, as commonly assumed previously, with relevant consequences for the dependence of neutron captures on metallicity (Busso et al. 1997). A thorough analysis of the implications of the new models is presented by BGW.

The stellar evolution results shown in this paper are all based on calculations performed with FRANEC (Frascati Raphson-Newton Evolutionary Code, see Chieffi & Straniero 1989). Stellar models appropriate for Population I stars have already been presented in Straniero et al. (1997) and Gallino et al. (1998); additional models have been computed specifically for the present paper. Our set of AGB models includes stars of masses from 1.5, 2, 3 and 5 M_{\odot} , and metallicity $Z = 0.006, 0.01$ and 0.02 . Mass-loss was taken into account adopting the parametrization by Reimers (1975) with values of the η parameter ranging from 0 to 5.

The FRANEC AGB models reproduce self-consistently the third dredge-up episode and the consequent mixing of freshly synthesized s -processed material (together with ${}^4\text{He}$ and ${}^{12}\text{C}$) to the surface of the star. According to Straniero et al. (1995, 1997) and Gallino et al. (1998), the third dredge-up starts after a limited number of thermal pulses, increasing its efficiency up to a maximum while the pulsing mechanism goes on, then decreases as mass loss and the advancement of the H-burning shell reduce the envelope mass, and eventually ceases when the latter decreases below about $0.5 M_{\odot}$.

The mass and the profile of the ${}^{13}\text{C}$ pocket were constrained by Busso et al. (1995, see also Busso et al. 1999) by comparing the results of neutron capture models with spectroscopically determined abundances in Population I AGB stars and in Population II Ba and CH stars with $[\text{Fe}/\text{H}] \leq -1$ (Smith & Lambert 1990; Luck & Bond 1991; Vanture 1992; Plez, Smith, & Lambert 1993). This was done by keeping constant the total mass of the ${}^{13}\text{C}$ pocket and parametrically varying the concentration of ${}^{13}\text{C}$ by factors from 0 to 2 times the profile indicated as “standard” (ST) by Gallino et al. (1998), corresponding for the choice

of the mass of the ^{13}C pocket made for this work to $3.1 \times 10^{-6} M_{\odot}$ of ^{13}C . As a result of this study, the ST choice for the ^{13}C pocket, when used in an AGB stellar model of metallicity $Z = Z_{\odot}/2$, was shown to reproduce remarkably well the abundance distribution of the solar main component (see also Arlandini et al. 1999, in preparation). However, AGB stars in the Galactic disk show a significant spread in their abundances of s -process elements (see discussion in Busso et al. 1995 and Busso et al. 1999). This spread can be attributed, at least in part, to variations in the ^{13}C profile, since the s -process efficiency depends strongly and non linearly on the local ^{13}C abundance. Following this indication, we have explored different extensions in mass of the ^{13}C pocket, while keeping for all metallicities the same ^{13}C profile as in ST case. We will later comment briefly on these choices. Let us mention here that the same choice was found to be appropriate to account for the s -process isotopic signatures of heavy elements (among which Ba, Nd, and Sm) in presolar grains most likely condensed in the circumstellar envelopes of AGB stars of solar metallicity (Gallino et al. 1993; Gallino et al. 1997) and recovered in meteoritic material (Ott & Begemann 1990; Prombo et al. 1993; Zinner 1997; Hoppe & Ott 1997).

At the end of the TP-AGB phase, the s -process contributions to the ISM are determined by the amount of matter cumulatively dredged-up from the He intershell to the surface and lost by stellar winds. This quantity is shown in Tab. 1 for the 2, 3, and 5 M_{\odot} stellar models and different metallicities (for the 5 M_{\odot} star we did not compute the model at $Z = 0.006$ but we doubled the cumulative dredged-up mass mixed into the envelope with respect to the solar case, in analogy with the results obtained for the 2 and 3 M_{\odot} cases).

In Fig. 1 we show the abundance by mass of Ba in the He shell material cumulatively mixed to the surface as a function of $[\text{Fe}/\text{H}]$ for a 2 M_{\odot} AGB model, for different assumptions on the total amount of ^{13}C nuclei present in the ^{13}C pocket. The dashed thick lines represent the extreme values chosen in the parametrization (0.17 and 1.33 times the ST case), whereas

TABLE 1

CUMULATIVE DREDGED-UP MASS IN THE ENVELOPE (IN M_{\odot}) FOR AGB STARS

Z	$2 M_{\odot}$	$3 M_{\odot}$	$5 M_{\odot}$
0.006	0.030	0.078	0.12
0.02	0.018	0.044	0.06

thin lines show intermediate cases. The thick continuous line represents the unweighted average yield calculated over all the cases shown. In Fig. 2 we show the full set of unweighted average yields for Ba, La, Ce, Nd, Pr, Sm, and Eu.

It is evident from Fig. 1 and 2 that there is a strong dependence of s -process yields on the initial stellar metallicity. This important result deserves additional comments. Since the build up of heavy nuclei requires neutron captures starting from Fe seeds, the s -process is expected to decline with declining metallicity, i.e. to be of *secondary* nature. However, the abundances produced depend not only on the initial Fe concentration, but also on the neutron exposure. The concentration of ^{13}C in the pocket is of *primary* nature (it is built from H and freshly made C, hence is independent of metallicity), while the abundance of the neutron absorber ^{56}Fe varies linearly with Z . Therefore the neutron exposure τ (roughly proportional to the ratio $^{13}\text{C}/^{56}\text{Fe}$) is expected to scale roughly as Z^{-1} . This dependence would compensate the mentioned secondary nature of the s -elements, if the yields of s -nuclei were linearly dependent on both τ and Z .

One has however to notice that the dependence of s -process yields on the neutron exposure is very complex and non linear (Clayton 1968). In general, the production factor of a given s -element (e.g. Ba) depends on the average abundances achieved by all the neutron-rich nuclei, and varies with Z also for metallicities close to solar. As shown in Fig. 1, in

the Galactic disk, for a range of metallicities covering about 1 dex, the strong increase of the s -process yields with increasing neutron exposure dominates and the secondary nature of these nuclei is *overcompensated*, so that they actually *increase* for decreasing Z , instead of remaining constant, as the previous simple discussion would have suggested.

At low metallicities, an important role is also played by light neutron absorbers, which are mainly primary in nature, as stressed by Clayton (1988) and by Mathews et al. (1992). Among these nuclei one has to include ^{12}C , ^{16}O and most of ^{22}Ne with its progeny. This is so because a large fraction of ^{22}Ne ultimately derives from the processing of the primary ^{12}C dredged-up into the envelope from the He-shell, which is transformed first to ^{14}N by shell H-burning and then to ^{18}O and ^{22}Ne by He-burning. Notice that the recently measured neutron capture cross section of one of the major primary neutron absorbers, ^{16}O (Igashira et al. 1995), is 170 times higher than the previous theoretical estimate quoted in Beer, Voss, & Winters (1992). On the whole, the importance of the moderating effect on the neutron density by all light neutron absorbers cannot be discarded.

In addition, as discussed by Gallino et al. (1998), radiative ^{13}C burning builds the distribution of s -elements in steps of relatively large n -exposition. This gives rise to higher values of the Ba/Zr ratio than feasible in any process working inside the pulses (that would produce simpler exponential n -exposure distributions). This last feature is a necessary condition for reproducing the abundance observations in CH giants near $[\text{Fe}/\text{H}] = -1$ (Vanture 1992; Busso et al. 1999) and also helps in maintaining a high production of Ba over a wide range of metallicities.

The trends shown in Fig. 2 can be understood through the interplay of the phenomena outlined above. Starting from AGB stars of nearly solar metallicity, first the s -fluence builds up the s -elements belonging to the Zr-peak, at neutron magic $N = 50$. Then the Zr-peak yields decrease while the Ba-peak production increases as shown in the Figure, reaching a

maximum at $[\text{Fe}/\text{H}] \simeq -0.6$. For lower metal contents, the n -flux skips Ba and feeds Pb, which reaches a maximum production yield at $[\text{Fe}/\text{H}] = -1$ (Gallino et al. 1999). Eventually, also Pb decreases making the secondary nature of the s -process evident. At these very low metallicities, essentially all the Fe group seeds are converted to Pb. Also thanks to the additional effect of light (primary) neutron absorbers, below $[\text{Fe}/\text{H}] \simeq -2$ only a very small s -signature is present on heavy elements.

3. Galactic chemical evolution model

Our model for the chemical evolution of the Galaxy is described in detail by Ferrini & Galli (1988), Galli & Ferrini (1989) and Ferrini et al. (1992). The model has been adopted to investigate different aspects of the chemical evolution of the Galaxy as well as global properties of external galaxies (see e.g. Mollà, Ferrini, & Díaz 1997 and references therein). Here we summarize its physical characteristics relevant to our study and briefly discuss the modifications to the original nucleosynthetic prescriptions introduced in the present work.

The Galaxy is divided into three zones, halo, thick disk, and thin disk, whose composition of stars, gas (atomic and molecular) and stellar remnants is computed as function of time up to the present epoch $t_{\text{Gal}} = 13$ Gyr. Stars are born with an initial composition equal to that of the gas from which they formed. The formation of the Sun takes place 4.5 Gyr ago, i.e. at epoch $t_{\odot} = 8.5$ Gyr. The thin disk is divided into concentric annuli, with no radial flow allowed, and is formed from material infalling from the thick disk and the halo. In the present work we neglect any dependence on galactocentric radius in the model results as well as in the observational data (see Mollà et al. 1997 for an application of the model to the study of radial abundance gradients), and we concentrate on the evolution inside the solar annulus, located 8.5 kpc from the Galactic center.

The star formation rate $\psi(t)$ is not assumed *a priori*, but is obtained as the outcome of self-regulating processes occurring in the molecular gas phase, either spontaneous or stimulated by the presence of other stars. The nucleosynthesis prescriptions are based upon the classic “matrix formalism” first introduced by Talbot & Arnett (1973). The mass of the element i ejected by a star of mass M after a time $\tau(M)$ from birth is assumed to be a linear combination of the masses of elements j initially present in the star:

$$M_i^{\text{ej}} = \sum_j Q_{ij} M_j^{\text{in}}, \quad (1)$$

where the matrix elements Q_{ij} depend on the mass and the metallicity of the star.

In the framework of Galactic evolution, it is convenient to consider separately the contribution of stars in different mass ranges. The model follows the evolution of (*i*) single low- and intermediate-mass stars ($0.8 M_\odot \leq M \leq M_\star$) ending their life as He or C-O white dwarf, (*ii*) binary systems able to produce Type I supernovae, and (*iii*) single massive stars ($M_\star \leq M \leq 100 M_\odot$), the progenitor of Type II supernovae. The value of M_\star depends on metallicity; we assume $M_\star = 6 M_\odot$ for $Z \leq 10^{-3}$ and $M_\star = 8 M_\odot$ otherwise (see for references Tornambè & Chieffi 1986). For each stellar group, the restitution rate $W_{i,k}(t)$ of element i is given by

$$W_{i,k}(t) = \int_{M_{\text{low}}}^{M_{\text{upp}}} \sum_j Q_{ij}[M, Z(t)] X_j[t - \tau(M)] \psi[t - \tau(M)] \phi(M) dM, \quad (2)$$

where the index k refers to the zone of the Galaxy, e.g. halo, thick disk and thin disk, and $X_j[t - \tau(M)]$ is the abundance (by mass) of element j in the ISM at the time of birth of a star of mass M . The adopted initial mass function $\phi(M)$ is discussed in Ferrini et al. (1992).

We have updated the nucleosynthesis prescriptions of Ferrini et al. (1992) for SNII and SNI adopting the yields computed by Woosley & Weaver (1995) and Thielemann, Nomoto, & Hashimoto (1996), respectively. As an example of the model results, Fig. 3a shows the run of star formation rate vs. $[\text{Fe}/\text{H}]$ in the three Galactic zones for our Standard Model

(corresponding to Model B of Pardi, Ferrini, & Matteucci 1995). The $[\text{Fe}/\text{H}]$ scale here is indicative of a time scale, albeit a non-linear one. The corresponding values of $[\text{O}/\text{Fe}]$ vs. $[\text{Fe}/\text{H}]$ for the three zones, computed with the revised yields, are plotted in Fig. 3b, together with an updated compilation of observational data. We have included abundance determinations obtained from measurements of the $[\text{OI}]$ forbidden lines (Gratton & Ortolani 1986; Barbuy 1988; Barbuy & Erdelyi-Mendes 1989; Sneden et al. 1991; Spite & Spite 1991; Edvardsson et al. 1993) and from the OH bands in the near UV (Israelian et al. 1998).

We see from Fig. 3a-b that the halo phase lasts approximately up to $[\text{Fe}/\text{H}] \lesssim -1.5$, the thick-disk phase covers the interval $-2.5 \lesssim [\text{Fe}/\text{H}] \lesssim -1$, and the thin-disk phase starts at approximately $[\text{Fe}/\text{H}] \gtrsim -1.5$. The slow decline of $[\text{O}/\text{Fe}]$ for increasing $[\text{Fe}/\text{H}]$, due to contribution of SNI as the evolution proceeds, is reproduced by the model over more than three decades in metallicity.

Recently Israelian, López, & Rebolo (1998) have measured oxygen abundances from the OH bands in the near UV in a sample of stars in the metallicity range $-3.0 < [\text{Fe}/\text{H}] < 0.3$ (also included in Fig. 3b). They found values significantly higher than those reported by other authors shown in the same Figure, with a continuous increase of $[\text{O}/\text{Fe}]$ with decreasing $[\text{Fe}/\text{H}]$. To reproduce these high values, one possibility is to increase the O contribution with respect to Fe of the most massive Type II SNe by a factor ~ 2 . This modification, of course, has no consequence on the chemical evolution of the *s*-process elements.

4. Results for the Galactic evolution of *s*- and *r*-elements

In this Section we present our results for the evolution of Ba, La, Ce, Nd, Pr, Sm and Eu in the Galaxy, by considering separately the *s*- and *r*-contributions. Then we compute the abundance of these elements resulting from the sum of the two processes and we com-

pare model results with the available spectroscopic observations of field stars at different metallicities.

4.1. Galactic *s*-process evolution

The *s*-process yields discussed in Sect. 2 and shown in Fig. 2 allow us to estimate the chemical enrichment of the Galaxy at different times. We show in Fig. 4 the resulting Ba *s*-fraction in the thin disk, compared with spectroscopic abundances obtained from various observational campaigns (Gratton & Sneden 1994; Woolf, Tomkin, & Lambert 1995; François 1996; McWilliam et al. 1998; Nissen & Schuster 1997; Norris, Ryan, & Beers 1997; Jehin et al. 1998; Mashonkina, Gehren, & Bikmaev 1999).

Though we have considered stars from 2 to 8 M_{\odot} , the mass range from which we get the dominant production of Ba is 2 – 4 M_{\odot} (as shown in Fig. 4), well representative of the most common low-mass AGB stars. More massive AGBs, in the range 4 – 8 M_{\odot} , do not give a relevant contribution to Ba-peak elements (see the following discussion).

As anticipated in Sect. 2, the direct comparisons of spectroscopic observations of AGB stars, solar system abundance determinations, isotopic anomalies in presolar SiC grains, with the predictions of stellar models constrain the mass of the ^{13}C pocket to within a certain range around a standard value. In the framework of Galactic chemical evolution, we adopt *averaged* stellar yields (shown in Fig. 1 and Fig. 2), calculated by assuming that all values of the ^{13}C pocket are equally probable within this interval. However, to test the sensitivity of our results to the choice of this fundamental parameter, we have also computed the Galactic evolution of the *s*-elements with stellar yields corresponding to the lower and upper bounds for the mass of the ^{13}C pocket. These aspects will be further discussed at the end of this subsection.

TABLE 2

s -PROCESS FRACTIONAL CONTRIBUTIONS (%) AT $t = t_{\odot}$

WITH RESPECT TO SOLAR SYSTEM ABUNDANCES

	case I ^(a)	case II ^(b)	case III ^(c)	KBW89 ^(d)
Ba	10	253	80	88
La	7	200	61	75
Ce	8	248	75	77
Pr	5	156	47	45
Nd	5	178	54	46
Sm	3	99	30	30
Eu	0.6	20	6	3

(a) – ^{13}C concentration: 0.17 times the ST case

(b) – ^{13}C concentration: 1.33 times the ST case

(c) – ^{13}C pocket mass averaged

(d) – Käppeler, Beer, & Wisshak (1989)

In Table 2 we list the resulting s -fractions (with respect to the corresponding solar abundances) at $t = t_{\odot}$. In the first two columns we show the results obtained using a mass of the ^{13}C pocket scaled by 0.17 (case I) and by 1.33 (case II) from the ST case. In the third column we show the results for the average yields (case III). The corresponding stellar yields are shown in Fig. 2 (case III), and, for Ba only, in Fig. 1 (case I, II and III). We also compare, in the fourth column, our results with the previous estimates by Käppeler, Beer, & Wisshak (1989), obtained with the so called *classical analysis*, based on model-independent analytical expressions (an exponential form) for the neutron irradiation. Notice that the results obtained with the extreme values of the mass of ^{13}C are in strong disagreement with either the results of the classical analysis or the observed solar abundances. As an illustration, we see from Table 2 that at $t = t_{\odot}$ the Ba s -fraction obtained with the average

yields is 80 % of the solar Ba abundance, whereas the lower and upper values of the mass of ^{13}C give a Ba s -fraction of 10 % and 253 %, respectively. Notice also that the average yields give results in reasonable agreement with the classical analysis.

It is evident from Fig. 4 that the s -process contribution dominates the Galactic evolution of Ba starting from $[\text{Fe}/\text{H}] \simeq -1.5$. At lower values of $[\text{Fe}/\text{H}]$, independently on the characteristics of the chemical evolution model, the contribution of s -process nucleosynthesis rapidly decreases due to the strong dependence of stellar yields on metallicity: *hence the contribution of low-mass AGB stars is far too low to account for the observed abundances in the range $-3 \lesssim [\text{Fe}/\text{H}] \lesssim -1.5$* . In order to check the sensitivity of this result on model inputs, we have considered the effects of the contribution of intermediate mass stars in the range $4\text{--}8 M_{\odot}$, adopting the yields of a $5 M_{\odot}$ AGB model with solar metallicity (Vaglio et al. 1999) as representative of this mass interval. These stars activate the $^{22}\text{Ne}(\alpha, n)^{25}\text{Mg}$ reaction during their TP-AGB phase more efficiently than in low-mass stars, because of the higher temperature reached at the bottom of the convective pulse ($T_{\text{max}} \lesssim 3.5 \times 10^8$ K). In contrast, the formation of a ^{13}C pocket is less certain, due to the reduced mass of the He intershell (by one order of magnitude). In this mass range the observational constraints are scarce and indirect: no AGB star of the Galaxy, for which we have a spectroscopic estimate of abundances, can be unambiguously attributed to this mass range, though in some post-AGB stars there is some suggestion that an intermediate mass star may have been the progenitor (Busso et al. 1999). Given such a lack of constraints, for these stars we have computed s -process nucleosynthesis induced by the $^{22}\text{Ne}(\alpha, n)^{25}\text{Mg}$ neutron source alone. We find that the neutron flux is too low for these stars to significantly contribute to the Galactic chemical evolution of the Ba-peak elements, whereas there is a consistent production of the elements belonging to the first s -peak: Sr, Y, and Zr. In particular, the contribution of intermediate mass stars only increase the Ba abundance at $t = t_{\odot}$ by about 3%, and let the rising of $[\text{Ba}/\text{Fe}]$ vs. $[\text{Fe}/\text{H}]$ shift at slightly lower metallicity, due to the shorter stellar lifetimes.

The results of the Galactic chemical evolution are not particularly sensitive to the value of the mass contained in the ^{13}C pocket adopted. For example, various tests for the s -process nucleosynthesis have been made by progressively reducing the ^{13}C mass giving results very close to the ones illustrated in Fig. 1. This is inherent to the s -process nucleosynthesis mechanism, which, increasing the number of available neutrons per Fe group seed (i.e. with decreasing metallicity), proceeds through the accumulation of neutron-magic nuclei, at $N = 50, 82, \text{ and } 126$, at the Zr-peak, Ba-peak and at Pb, respectively. Varying the total mass involved in the ^{13}C pocket in the present calculations by a factor of 2 is equivalent to vary by only 30 % the final yield, because of the overlapping mechanisms between subsequent pulses. This is an indication to extend the analysis to cases with somewhat higher abundances of ^{13}C nuclei with respect to the upper case ($1.3 \times \text{ST}$) considered in the present calculations, as suggested by the comparison of spectroscopic abundances of some s -enhanced stars (Busso et al. 1999).

Despite the large number of approximations (the total amount of dredged-up material, which depends on the stellar evolutionary code and on the adopted law of mass loss by stellar winds, the parametrization on the ^{13}C pocket, etc.) the present results appear to reasonably reproduce the s -process distribution of the heavy elements, from the Ba-peak up to Pb (see also Gallino et al. 1998, 1999).

4.2. Galactic r -process contribution

As first suggested by Truran (1981), the presence of r -process elements in low metallicity halo stars (Gratton & Sneden 1994; McWilliam et al. 1995; McWilliam 1998) is indicative of a prompt enrichment of the Galaxy in these elements, possibly by early generations of massive stars.

It is possible to constrain quantitatively the enrichment of r -process elements in the ISM during the evolution of the Galaxy on the basis of the results presented in Sect. 4.1 and in Table 2 for the s -process contribution at $t = t_{\odot}$. The so-called r -process residuals are obtained by subtracting the s -process contribution N_s/N_{\odot} from the fractional abundances in the solar system taken from Anders & Grevesse (1989):

$$N_r/N_{\odot} = (N_{\odot} - N_s)/N_{\odot}. \quad (3)$$

In the case of Ba we obtain a r -residual of 20%. The assumption that the r -process is of primary nature and originates from massive stars allows us to estimate the contribution of this process during the evolution of the Galaxy. In the case of Ba, for example, we have

$$\left(\frac{\text{Ba}}{\text{O}}\right)_{r,\odot} \simeq 0.2 \left(\frac{\text{Ba}}{\text{O}}\right)_{\odot}. \quad (4)$$

Since the s -process does not contribute at low metallicity (see Sect. 4.1 and Fig. 4), for Population II stars we have approximately

$$\left(\frac{\text{Ba}}{\text{O}}\right) \simeq \left(\frac{\text{Ba}}{\text{O}}\right)_{r,\odot}, \quad (5)$$

which yields

$$\left[\frac{\text{Ba}}{\text{Fe}}\right] = \left[\frac{\text{Ba}}{\text{O}}\right] + \left[\frac{\text{O}}{\text{Fe}}\right] \simeq \log(0.2) + 0.6 \simeq -0.1 \text{ dex}, \quad (6)$$

assuming a typical $[\text{O}/\text{Fe}] \simeq 0.6$ dex for Population II stars. Thus, the r -process contribution for $[\text{Fe}/\text{H}] \lesssim -1.5$ dominates over the s -contribution and roughly reproduces the observed values. The simple argument presented here ignores, however, the effects of the finite lifetimes of stars, the distribution of stellar masses, and the time dependence of the star formation rate. All these effects are instead taken into account in our chemical evolution model. The results shown in Fig. 5 for Ba and Eu confirm the estimate given above, and provide a strong constraint on the mass range of SNII contributing to r -process nucleosynthesis. In fact, the characteristic decline of $[r/\text{Fe}]$ as function of $[\text{Fe}/\text{H}]$ suggested by observations of

metal-poor stars (Cowan, Thielemann, & Truran 1991; Mathews et al. 1992; Gratton & Sneden 1994) can be naturally explained by a time delay between the O-rich (and partly Fe-rich) material ejected by the more massive SNII ($M \geq 15 M_{\odot}$), and r -process material ejected by the lower mass SNe. This delay may reflect the actual difference in stellar lifetimes, but can be amplified by non-instantaneous mixing processes in the ISM. As for the scatter of spectroscopic data at very low metallicities, this problem will be discussed in the next subsection.

In particular we have considered in Fig. 5 the following cases: (a) the full range of SNII, (b) SNII in the mass interval $10 \leq M/M_{\odot} \leq 12$, and (c) SNII in the mass interval $8 \leq M/M_{\odot} \leq 10$. It is evident that in order to reproduce the typical increasing trend of [Ba/Fe] or [Eu/Fe] at $[\text{Fe}/\text{H}] \lesssim -1.5$, the production of Fe at low metallicity must have occurred substantially before the production of the r -process component of Ba and Eu. According to our model, SNII in the mass range $8 \leq M/M_{\odot} \leq 10$ appear to be good candidates for the *primary* production of r -nuclei, whereas a range extended to much higher masses seems to give results in conflict with the available observations. We note in addition that the identification of low-mass SNe as a possible site for the r -process is also supported by recent theoretical SN models by Wheeler et al. (1998), Freiburghaus et al. (1998), and Meyer & Brown (1997).

4.3. s - and r -process contributions to Galactic chemical evolution

In this Section we present our results for the Galactic chemical evolution of elements from Ba to Eu, based on the assumptions discussed in Sect. 4.1 – 4.2, namely that the s -process contribution to the production of these elements comes from $2 - 4 M_{\odot}$ AGB stars, and the r -process contribution originates from SN in the range $8 - 10 M_{\odot}$.

Fig. 6 to 11 show the Galactic evolution of Ba, La, Ce, Nd, Pr, Sm, computed by adding the s - and r -process contributions (abundances are given with respect to Fe and Eu in the upper and lower panels respectively). Fig. 12 shows the resulting evolution of $[\text{Eu}/\text{Fe}]$ as a function of $[\text{Fe}/\text{H}]$, compared with spectroscopic abundances determined in dwarf and giant stars of different metallicities.

The $[\text{element}/\text{Fe}]$ ratios (upper panels of Fig. 6 – 11) provide information about the enrichment relative to Fe in the three Galactic zones, making clear that a delay in the r -process production with respect to Fe is needed in order to match the spectroscopic data in the range $-3 \lesssim [\text{Fe}/\text{H}] \lesssim -2$. The observations show that the $[\text{element}/\text{Fe}]$ ratios begin to decline in metal-poor stars, with a sharp drop at $[\text{Fe}/\text{H}] \lesssim -2.5$. This trend can be naturally explained by the finite lifetimes of stars at the lower end of the adopted mass range: massive stars in the early times of the evolution of the Galaxy evolve quickly, ending as SNII producing O and Fe. Later, less massive stars explode as SNII, producing r -process elements and causing the sudden increase in $[\text{element}/\text{Fe}]$.

Since Eu is mostly produced by r -process nucleosynthesis (94% at $t = t_{\odot}$, see Tab. 2), the $[\text{element}/\text{Eu}]$ abundance ratios (bottom panels) provide a direct way to judge the relative importance of the s and r channels during the evolution of the Galaxy. According to our model, at low metallicity the r -process contribution is dominant, and the $[\text{element}/\text{Eu}]$ ratio is approximately given by the element’s r -fraction computed with the r -residuals discussed in Sect. 4.2. On the contrary, for $[\text{Fe}/\text{H}] \gtrsim -1.5$, the s -process contribution takes over, and the $[\text{element}/\text{Eu}]$ ratios rapidly increase approaching the solar values. This trend is particularly evident in the observational data for Ba and Ce, as these elements have the largest s -process contribution.

The agreement of the model results with observational data for s -process dominated elements (e.g. Ba and Ce) provides a strong support to the validity of the nucleosynthesis

prescriptions adopted in this work and AGB modelings with the FRANEC code, including the estimate of the s -process and ^{12}C -rich material dredged-up in AGB envelopes and eventually mixed with the ISM by stellar winds. In turn, the s -fractions obtained from our model at $t = t_{\odot}$, listed in Table 2, are used to normalize the r -process nucleosynthesis and therefore determine the element abundances at earlier Galactic epochs. In addition, a few points should be noticed.

First, at high metallicities, the abundances of La, Nd, and Sm with respect to Fe are slightly overestimated as compared to spectroscopic observations, whereas the ratios to Eu are well reproduced. On the other hand, for Ba, Ce, and Pr, the predicted abundance ratios with respect to Fe are in good agreement with the observational data, whereas the ratios with respect to Eu appears to be slightly underestimated. The origin of discrepancies in the [element/Fe] ratio might be attributed to specific characteristics of the Galactic evolution model (e.g. the Fe production by SNI/SNII). The ratio [element/Eu], however, is much less model dependent, and discrepancies between model results and observations should be attributed more likely to incomplete observational data.

Second, europium deserves a particular attention as it is one of the few r -process elements that has clean atomic lines accessible in the visible part of the spectrum, which makes it an important diagnostic of the r -process history of stellar material. In Fig. 12 we show the observationally determined values of [Eu/Fe] in a sample of halo and disk stars. For $[\text{Fe}/\text{H}] \geq -2.4$, the similarity of O and Eu trends vs. $[\text{Fe}/\text{H}]$ strongly supports the idea of a common production site, presumably SNII. In the same Fig. 12 we also show the results of our chemical evolution model, obtained following the prescriptions described in Sect. 4.2. The scatter in [Eu/Fe] at lower metallicities (also observed in the other Ba-peak elements) can be ascribed to an incomplete mixing in the Galactic halo gas, allowing the formation of stars super-rich in r -process elements, like CS 22892-052 (see Sneden et al. 1996). This star

in particular, with $[\text{Fe}/\text{H}] \simeq -3.1$, shows r -process enhancements of 40 times the solar value (e.g. $[\text{Eu}/\text{Fe}] \simeq +1.7$, and $[\text{Ba}/\text{Fe}] \simeq +0.9$), much larger than the abundances observed in any normal halo star. Nevertheless its $[\text{Ba}/\text{Eu}]$ is in good agreement with the typical r -process ratios we predict at this metallicity. Therefore CS 22892-052 is likely to be a star born in an environment more strongly polluted by supernova debris than the average halo gas; its peculiar abundances support the idea of an inhomogeneous composition of the halo at early times.

Third, at low metallicity, the values of $[\text{element}/\text{Fe}]$ shown in Fig.6 – 11 suggest an *intrinsic* scatter over about 2 dex. McWilliam et al. (1995) and McWilliam (1998) have argued that the observed dispersion in heavy element abundances at low metallicity entirely reflects the actual inhomogeneities in the chemical composition of the gas from which these extremely metal-poor halo stars were formed. Ryan, Norris, & Beers (1996) took a step further and speculated that the resulting chemical enrichment of the gas would be highly inhomogeneous and basically limited to the supernova’s sphere of influence. The problem of the observed spread in the measured stellar abundances, in connection with mixing of heavy elements in the various Galactic zones is a complicated one, and in our opinion not fully understood. The spread observed in the Galactic disk population by Edvardsson et al. (1993) may result either from the multizone structure of the Galaxy (the thick and thin disk contribute in different ways to the local enrichment), or from a contamination of contiguous radial zones (see Mollà et al. 1997 for details). In the halo, the non locality of observed populations will be again a good reason for a relevant spread in the abundance distribution. The question remains if these mechanisms can be responsible for the extremely large spread in the spectroscopic data presented by McWilliam (1998).

We must keep in mind that models of Galactic chemical evolution often assume instantaneous mixing between stellar ejecta and the ISM, and they can therefore provide only

spatially averaged values of element abundances as a function of time and galactocentric distance. While such an assumption is justified during the evolution of the Galactic disk and the late times of the halo phase, a different kind of approach should be taken when investigating the earliest phases of halo enrichment, where a coupled treatment of the chemistry and the dynamics of the gas, both on a large scale (collapse) and on a small scale (supernovae), is needed for a more realistic modeling. Preliminary results concerning Ba are shown in Cravanzola et al. (1999), where the chemo-dynamical evolution of the Galaxy is followed by means of a N-body/SPH code. Similar conclusions have been advanced by Ishimaru & Wanajo (1999).

On the other hand, the consistent observational scatter at very low metallicities can be attributed, at least in part, to uncertainties in the spectroscopic observations, which suffer for poor signal-to-noise ratios due to the intrinsic weakness of the sources (Gratton & Sneden 1994; Gratton 1995).

The *s*-process contributions to the various isotopes of the elements considered in this paper are listed in Table 3. For example, at $t = t_{\odot}$ the model can account for 94% and 97% of the *s*-only isotopes ^{134}Ba and ^{136}Ba , respectively. The dominantly *r*-process Eu isotopes are affected by the *s*-process only at the 5% level. The solar distribution of *s*- and *r*-fractions of individual isotopes is reproduced within $\sim 10\%$.

5. Conclusions

In this paper we have calculated the evolution of *n*-capture elements from Ba to Eu in the interstellar gas of the Galaxy. The input stellar yields for neutron-rich nuclei have been separated into their *s*- and *r*-process components. We have obtained the *s*-yields with post-process calculations based on AGB models computed with the FRANEC code. The

TABLE 3

s-PROCESS FRACTIONAL CONTRIBUTIONS (%) FOR ISOTOPES FROM BA TO EU
AT $t = t_{\odot}$ WITH RESPECT TO SOLAR SYSTEM ABUNDANCES

^{134}Ba	94	^{141}Pr	47	^{147}Sm	20
^{135}Ba	22	^{142}Nd	93	^{148}Sm	96
^{136}Ba	97	^{143}Nd	30	^{149}Sm	12
^{137}Ba	58	^{144}Nd	48	^{150}Sm	94
^{138}Ba	84	^{145}Nd	26	^{152}Sm	21
^{139}La	61	^{146}Nd	61	^{154}Sm	0.5
^{140}Ce	81	^{148}Nd	13	^{151}Eu	6
^{142}Ce	12	^{150}Nd	0.02	^{153}Eu	5

results of the Galactic evolution model, compared with spectroscopic observations of F and G dwarf stars, confirm the basic nucleosynthesis scenario outlined by Straniero et al. (1997) and Gallino et al. (1998). The ^{13}C neutron source, active during the interpulse phases of low-mass TP-AGB stars, accounts for most of the *s*-process contribution to elements from Ba to Eu. In the Galactic disk the abundance of Ba is dominated by the *s*-process for $[\text{Fe}/\text{H}] \gtrsim -1.5$. At lower metallicities, the primary *r*-process contribution, relatively small at the time of formation of the Sun (20% of solar Ba), plays a dominant role.

Concerning the enrichment of the Galaxy in the *r*-process elements, the comparison of the predictions of the Galactic chemical model with the available spectroscopic data for Population II stars suggests a production from SNII slightly delayed with respect to the main phase of oxygen enrichment. The overall decline of $[r/\text{Fe}]$ vs. $[\text{Fe}/\text{H}]$ in the most metal-poor stars can be explained if the *r*-process derives from core-collapse SNe at the lowest stellar mass limit, around 8–10 M_{\odot} .

The Galactic evolution of the lighter s -process nuclei (e.g. Sr, Y, Zr) as well as of Pb will be presented in a forthcoming paper. Spectroscopic determinations of the abundance of these elements in Galactic halo stars are currently under way (see e.g. Sneden et al. 1998 for recent HST data). Concerning Pb, preliminary results on the s -fraction at $t = t_{\odot}$ and on its sharp increase at low metallicities, confirm the prediction by Gallino et al. (1998) that the production of ^{208}Pb (the *strong component*) has to be entirely attributed to s -process occurring in low-metallicity, low-mass AGB stars.

We would like to thank C. Arlandini, A. Chieffi, M. Limongi and M. Lugaro for useful discussions. We also thank S. Sandrelli and U. Penco for kind assistance with the numerical calculations. The work of C.T. and D.G. is supported in part by grant Cofin98-MURST at the Osservatorio Astrofisico di Arcetri. The work of R.G. and M.B. is supported by grant Cofin98-MURST at the Dipartimento di Fisica Generale, Università di Torino, and Osservatorio Astronomico di Pino Torinese.

REFERENCES

- Anders, E., & Grevesse, N. 1989, *Geochim. Cosmochim. Acta*, 53, 197
- Andreani, P., Vangioni-Flam, E., & Audouze, J. 1988, *ApJ*, 334, 698
- Barbuy, B. 1988, *A&A*, 191, 121
- Barbuy, B., & Erdelyi-Mendes, M. 1989, *A&A*, 214, 239
- Beer, H., Voss, F., & Winters, R.R. 1992, *ApJS*, 80, 403
- Blanco, V.M., McCarthy, M.F., & Blanco, B.M. 1980, *ApJ*, 242, 938
- Burbidge, E.M., Burbidge, G.R., Fowler, W.A., Hoyle, F. 1957, *Rev. Mod. Phys.*, 29, 547
- Busso, M., Picchio, G., Gallino, R., & Chieffi, A. 1988, *ApJ*, 326, 196
- Busso, M., Lambert, D.L., Gallino, R., Beglio, L., Raiteri, C.M., & Smith, V.V. 1995, *ApJ*, 446, 775
- Busso, M., Travaglio, C., Gallino, R., Lugaro, M., & Arlandini, C. 1999, in *Nuclei in the Cosmos V*, ed. N. Prantzos, (Paris: Edition Frontières), in press
- Busso, M., Gallino, R., & Wasserburg, G. J. 1999, *ARA&A*, in press (BGW)
- Cameron, A.G.W. 1954, *Phys. Rep.*, 93, 932
- Caughlan, G.R., & Fowler, W.A. 1988, *Atom. Data. Nucl. Data Tables*, 40, 283
- Chieffi, A., & Straniero, O. 1989, *ApJS*, 71, 47
- Clayton, D.D., 1968, *Principles of Stellar Structure and Nucleosynthesis*, (Chicago: University of Chicago Press)
- Clayton, D.D. 1988, *MNRAS*, 234, 1

- Clayton, D.D., & Ward, R.A. 1974 *ApJ*, 193, 397
- Clegg, R., Lambert, D.L., & Bell, R.A. 1979, *ApJ*, 234, 188
- Cowan, J.J., Thielemann, F.K., & Truran, J.W. 1991, *ARA&A*, 29, 447
- Cravanzola, A., Raiteri, C.M., Villata, M., & Gallino, R. 1999, in *Nuclei in the Cosmos V*, ed. N. Prantzos, (Paris: Edition Frontières), in press
- Denker, A., Drotleff, H.W., Grosse, M., Knee, H., Kunz, R., et al. 1995, in *Nuclei in the Cosmos III*, ed. M. Busso, C.M. Raiteri, & R. Gallino, *AIP Conf. Proc.*, 327, (New York: AIP), p. 255
- Despain, K.H. 1980, *ApJ*, 236, 648
- Edvardsson, B., Andersen, J., Gustaffson, B., Lambert, D.L., Nissen, P.E., & Tomkin, J. 1993, *A&A*, 275, 101
- Ferrini, F., & Galli, D. 1988, *A&A*, 195, 27
- Ferrini, F., Matteucci, F., Pardi, C., & Penco, U. 1992, *ApJ*, 387, 138
- François, P. 1996, *A&A*, 313, 229
- Freiburghaus, C., Rembges, J.F., Rauscher, T., Thielemann, F.K., Kratz, K.L., Pfeiffer, B., & Cowan, J.J. 1998, *ApJ*, in press
- Galli, D., & Ferrini, F. 1989, *A&A*, 218, 31
- Gallino, R., Raiteri, C.M., & Busso, M. 1993, *ApJ*, 410, 400
- Gallino, R., Busso, M., & Lugaro, M. 1997, in *Astrophysical Implications of the Laboratory Study of Presolar Materials*, eds. T. Bernatowicz & E. Zinner, (New York: AIP), p. 115

- Gallino, R., Arlandini, C., Busso, M., Lugaro, M., Travaglio, C., Straniero, O., Chieffi, A., & Limongi, M. 1998, *ApJ*, 497, 388
- Gallino, R., Busso, M., Lugaro, M., Travaglio, C., Arlandini, C., & Vaglio, P. 1999, in *Nuclei in the Cosmos V*, ed. N. Prantzos, (Paris: Edition Frontières), in press
- Gilroy, K.K., Sneden, C., Pilachowski, C.A., & Cowan, J. 1988, *ApJ*, 327, 298
- Gratton, R. 1995, in *Nuclei in the Cosmos III*, ed. M. Busso, R. Gallino, & C.M. Raiteri, (New York: AIP), p. 3
- Gratton, R., & Ortolani, S. 1986, *A&A*, 169, 201
- Gratton, R., & Sneden, C. 1994, *ApJ*, 287, 927
- Herwig, F., Blöcker, T., Schönberner, D., & El Eid, M. 1997, *A&A*, 324, L81
- Hollowell, D.E., & Iben, I.Jr. 1988, *ApJ*, 333, L25
- Hollowell, D.E., & Iben, I.Jr. 1989, *ApJ*, 340, 966
- Hoppe, P., & Ott, U. 1997, in *Astrophysical Implications of the Laboratory Study of Presolar Materials*, ed. Th.J. Bernatowicz & E. Zinner (New York: Woodbury), p. 27
- Howard, W.M., Mathews, G.J., Takahashi, K., & Ward, R.A. 1986, *ApJ*, 309, 633
- Iben, I.Jr., & Truran, J.W. 1978, *ApJ*, 220, 980
- Iben, I.Jr., & Renzini, A. 1982a, *ApJ*, 263, L23
- Iben, I.Jr. 1982, *ApJ*, 260, 821
- Iben, I.Jr. 1983, *ApJ*, 275, L65
- Igashira, M., Nagai, Y., Masuda, K., Ohsaki, T., & Kitazawa, H. 1995, *ApJ*, 441, L89

- Israelian, G., García López, R.J., & Rebolo, R. 1998, *ApJ*, 507, 805
- Ishimaru, Y., & Wanajo, S. 1999, *ApJ*, 511, L33
- Jehin, E., Magain, P., Neuforge, C., Noels, A., Parmentier, G., & Thoul, A.A. 1998, *astro-ph/9809405*
- Käppeler, F., Beer, H., Wisshak, K., Clayton, D.D., Macklin, R.L., & Ward, R.A. 1982, *ApJ*, 257, 821
- Käppeler, F., Beer, H., & Wisshak, K. 1989, *Rep. Prog. Phys.*, 52, 945
- Lamb, S.A., Howard, W.M., Truran, W.A., & Iben, I.Jr. 1977, *ApJ*, 217, 213
- Lambert, D. 1991, in *Evolution of Stars: the Photospheric Abundance Connection*, ed. G. Michaud & A. Tutukov (Dordrecht: Kluwer), p. 299
- Langer, N., Heger, A., Woosley, S.E., & Herwig, S. 1999, in *Nuclei in the Cosmos V*, ed. N. Prantzos, (Paris: Edition Frontières), in press
- Luck, R.E., & Bond, H.E. 1991, *ApJS*, 77, 515
- Malaney R.A. 1986, *MNRAS*, 223, 683
- Mashonkina, L., Gehren, T., & Bikmaev, I. 1999, *A&A*, 343, 519
- Mathews, G.J., Bazan, G., & Cowan, J.J. 1992, *ApJ*, 391, 719
- McWilliam, A. 1995, *ARA&A*, 35, 503
- McWilliam, A., Preston, G.W., Sneden, C., & Searle, L. 1995, *AJ*, 109, 2757
- McWilliam, A. 1998, *AJ*, 115, 1640
- Meyer, B.S. 1994, *ARA&A*, 32, 153

- Meyer, B.S., & Brown, J.S. 1997, *ApJS*, 112, 199
- Mollá, M., Ferrini, F., Díaz, A.I. 1997, *ApJ*, 475, 519
- Norris, J.E., Ryan, S.G., & Beers, T.C. 1997, *ApJ*, 489, L169
- Ott, U., & Begemann, F. 1990, *ApJ*, 353, L57
- Pardi, M.C., Ferrini, F., & Matteucci, F. 1995, *ApJ*, 444, 207
- Plez, B., Smith, V.V., & Lambert, D.L. 1993, *ApJ*, 418, 812
- Prantzos, N., Hashimoto, M., Rayet, M., & Arnould, M. 1990, *A&A*, 238, 455
- Prombo, C., Podosek, F., Amari, S., Lewis, R.S. 1993, *ApJ*, 410, 393
- Raiteri, C.M., Gallino, R., Busso, M., Neuberger, D., & Käppeler, F. 1993, *ApJ*, 419, 207
- Reimers, D. 1975, in *Problems in Stellar Atmospheres and Envelopes*, ed. B. Baschek, H. Kegel, & G. Traving, (Berlin: Springer), p. 229
- Ryan, S.G., Norris, J.E., & Beers, T.C. 1996, *ApJ*, 471, 254
- Singh, H.P., Roxburgh, I.W., & Chan, K.L. 1998, *A&A*, 340, 178
- Smith, V.V., & Lambert, D.L. 1986, *ApJ*, 311, 843
- Smith, V.V., & Lambert, D.L. 1990, *ApJS*, 72, 387
- Snedden, C., & Parthasarathy, M. 1983, *ApJ*, 267, 757
- Snedden, C., Kraft, R., Prosser, C.F., & Langer, G.E. 1991, *AJ*, 102, 2001
- Snedden, C., McWilliam, A., Preston, W., Cowan, J.J., Burris, D.L., & Armosky, B.J. 1996, *ApJ*, 467, 819

- Snedden, C., Cowan, J.J., Burris, D.L., & Truran, J.W. 1998, *ApJ*, 496, 235
- Spite, M., & Spite, F. 1978, *A&A*, 67, 23
- Spite, M., & Spite, F. 1991, *A&A*, 252, 689
- Straniero, O., Chieffi, A., Limongi, M., Busso, M., Gallino, R., & Arlandini, C. 1997, *ApJ*, 478, 332
- Straniero, O., Gallino, R., Busso, M., Chieffi, A., Raiteri, C.M., Salaris, M., & Limongi, M. 1995, *ApJ*440, L85
- Talbot, R.J., & Arnett, D.W. 1973, *ApJ*, 186, 51
- Thielemann, F.-K., Nomoto, K., & Hashimoto, M. 1996, *ApJ*, 460, 408
- Tornambè, A., & Chieffi, A. 1986, *MNRAS*, 220, 529
- Truran, J.W., & Iben, I.Jr. 1977, *ApJ*, 216, 797
- Truran, J.W. 1981, *A&A*, 97, 391
- Vaglio, P., Gallino, R., Busso, M., Travaglio, C., Straniero, O., Chieffi, A., Limongi, M., Arlandini, C., & Lugaro, M. 1999, in *Nuclei in the Cosmos V*, ed. N. Prantzos, (Paris: Edition Frontières), in press
- Vanture, A.D. 1992, *AJ*, 104, 1986
- Wasserburg, G.J., Busso, M., & Gallino, R. 1996, *ApJ*, 466, L109
- Wheeler, J.C., Sneden, C., & Truran, J.W. 1989, *ARA&A*, 97, 391
- Wheeler, J.C., Cowan, J.J., & Hillebrandt, W. 1998, *ApJ*, 493, L101
- Wolf, V.M., Tomkin, J., & Lambert, D. 1995, *ApJ*, 453, 660

Woosley, S.E., Wilson, J.R., Mathews, G.J., Hoffman, R.D., & Meyer, B.S. 1994, ApJ, 433,
229

Woosley, S.E., & Weaver, T.A. 1995, ApJS, 101, 181

Zinner, E. 1997, in Astrophysical Implications of the Laboratory Study of Presolar Materials,
ed. Th.J. Bernatowicz & E. Zinner (New York: Woodbury), p. 3

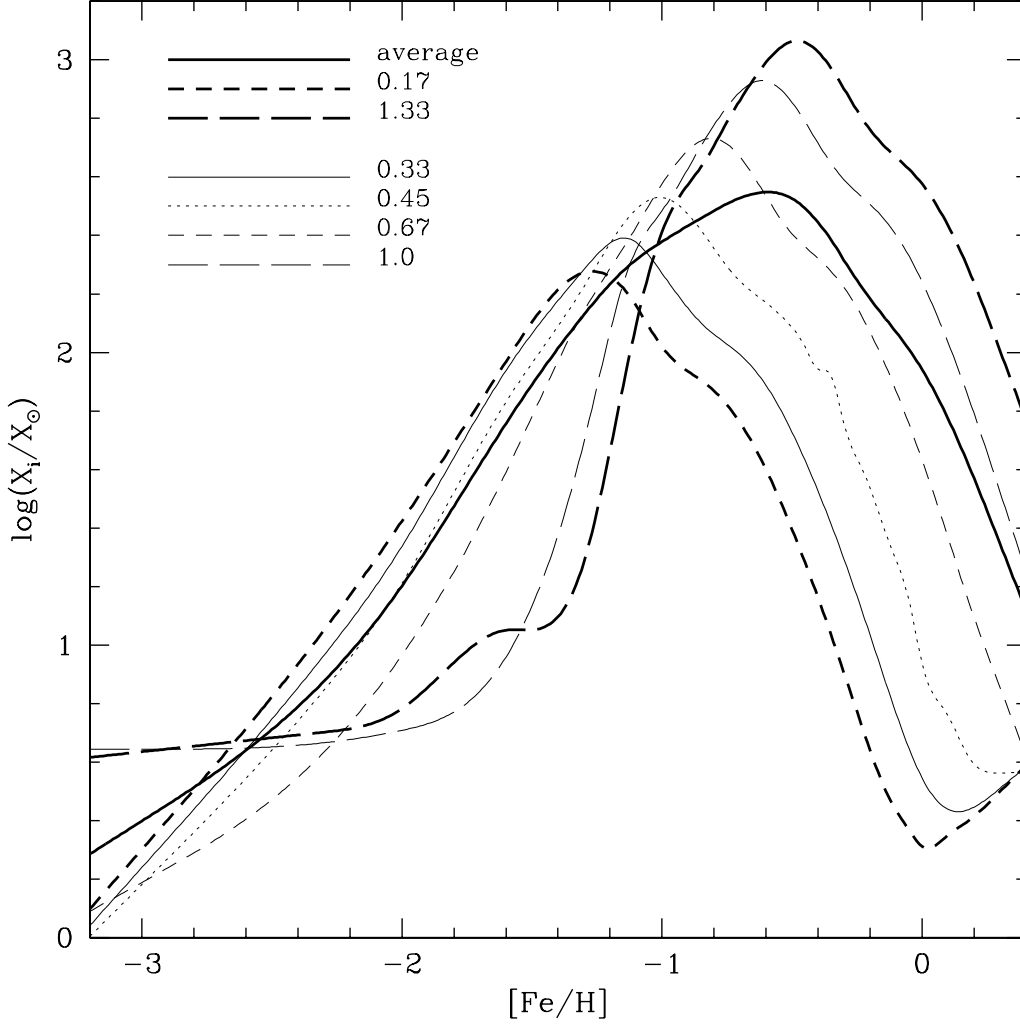


Fig. 1.— Abundances by mass (relative to solar) of Ba in the material cumulatively mixed to the surface of a $2 M_{\odot}$ star by third dredge-up episodes as function of metallicity, for different assumptions on the mass of the ^{13}C pocket. The *short-* and *long-dashed thick lines* represent the cases 0.17 and 1.33 times the standard value (see text) respectively, whereas the *thin lines* show intermediate cases (0.33, 0.45, 0.67, and 1 times the standard value). The *thick continuous line* represents the unweighted average of all cases shown.

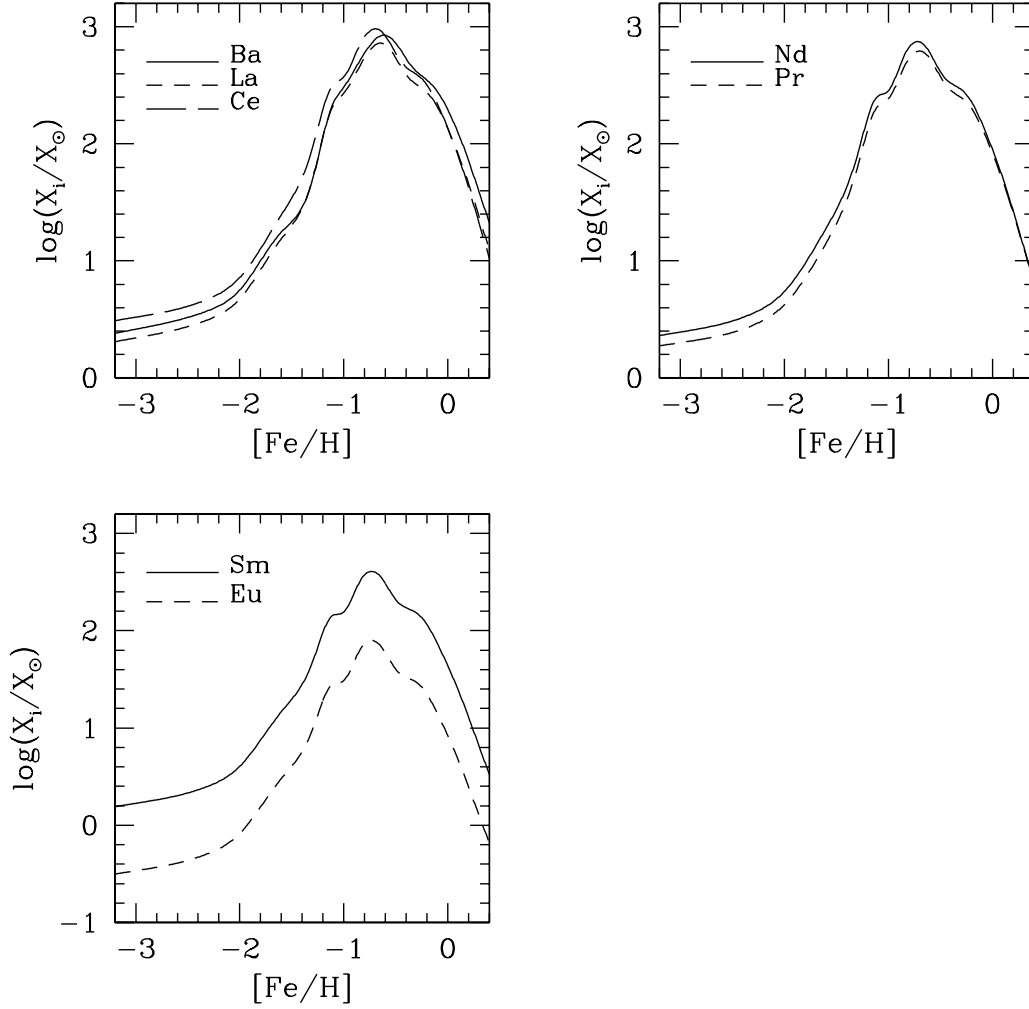


Fig. 2.— Abundances by mass (relative to solar) of Ba, La, and Ce (*top left panel*), Nd and Pr (*top right panel*), Sm and Eu (*bottom left panel*) in the material cumulatively mixed to the surface of a $2 M_\odot$ star by third dredge-up episodes as function of metallicity.

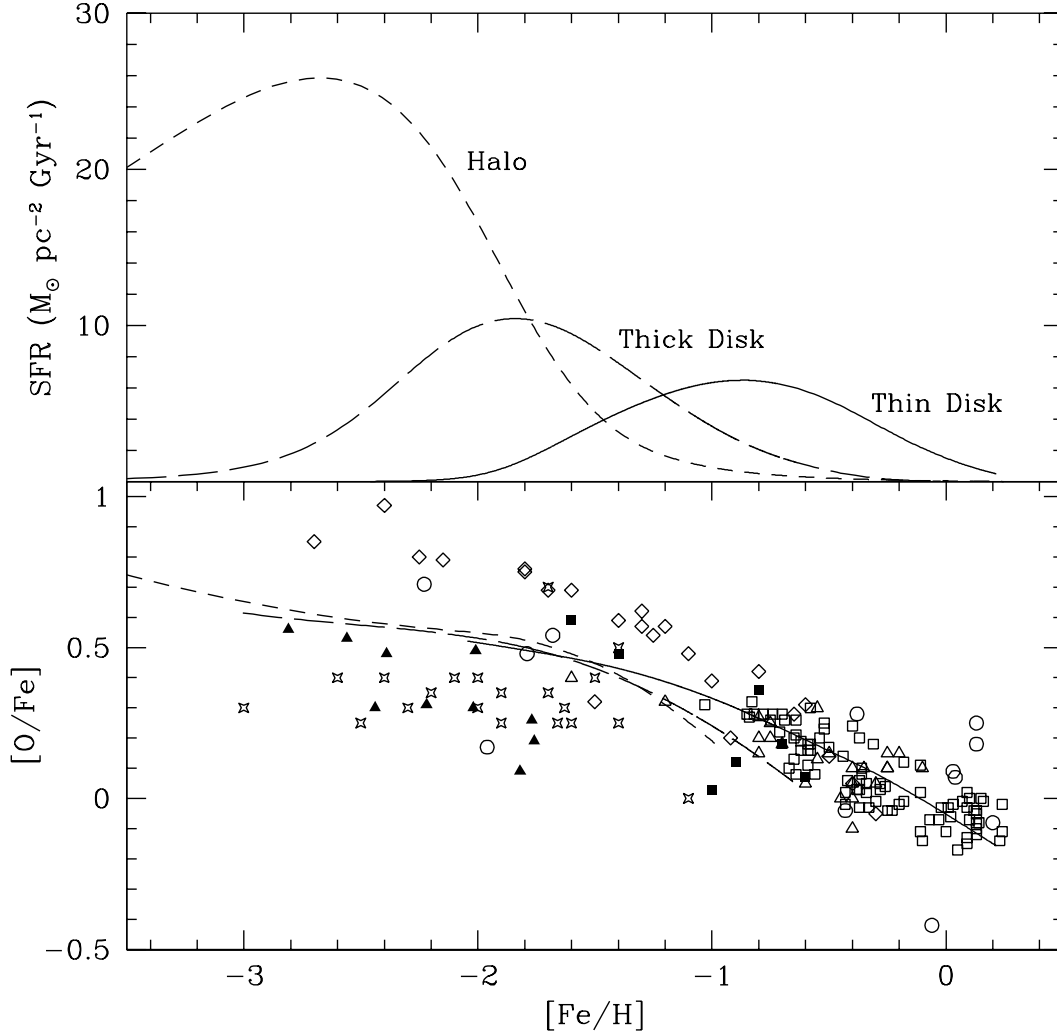


Fig. 3.— Star formation rate (*upper panel*) and $[\text{O}/\text{Fe}]$ (*lower panel*) according to our standard model of Galactic evolution, displayed as function of $[\text{Fe}/\text{H}]$. $[\text{O}/\text{Fe}]$ predictions are compared with spectroscopic observations by: Gratton & Ortolani (1986) (*circles*); Barbuy (1988) (*open triangles*); Barbuy & Erdelyi-Mendes (1989) (*four-pointed stars*); Sneden et al. (1991) (*filled triangles*); Spite & Spite (1991) (*filled squares*); Edvardsson et al. (1993) (*open squares*); Israelian et al. (1998) (*diamonds*).

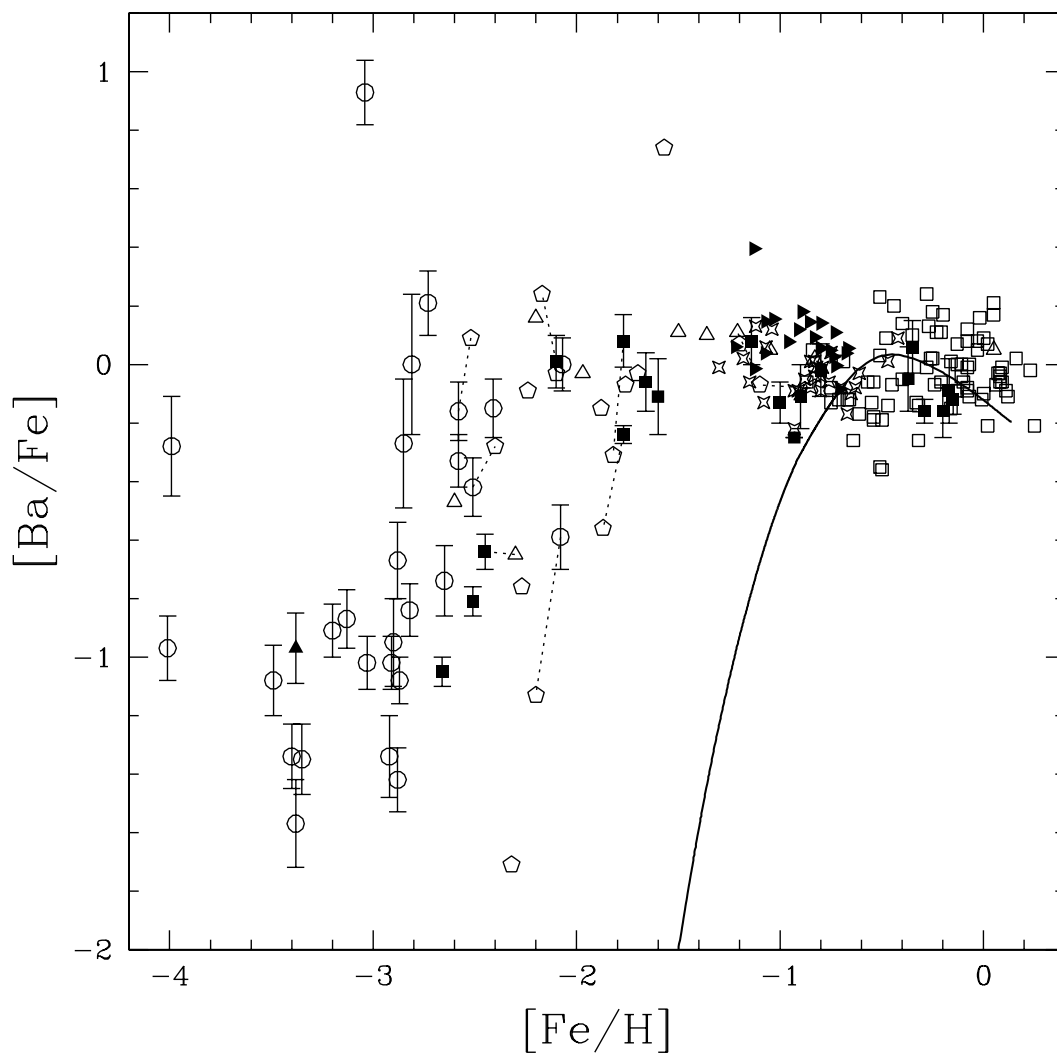


Fig. 4.— Evolution of Ba s -fraction in the thin disk as function of $[\text{Fe}/\text{H}]$ according to our standard model (*solid line*). Observational data are from Gratton & Sneden (1994) (*filled squares*); Woolf et al. (1995) (*open squares*); François (1996) (*pentagons*); McWilliam et al. (1995) and McWilliam (1998) (*circles*); Norris et al. (1997) (*filled triangles*); Jehin et al. (1998) (*filled tilted triangles*); Mashonkina et al. 1999 (*open triangles*). Thin dotted lines connect stars with different abundance determinations. Errorbars are shown only when

reported by the authors for single objects.

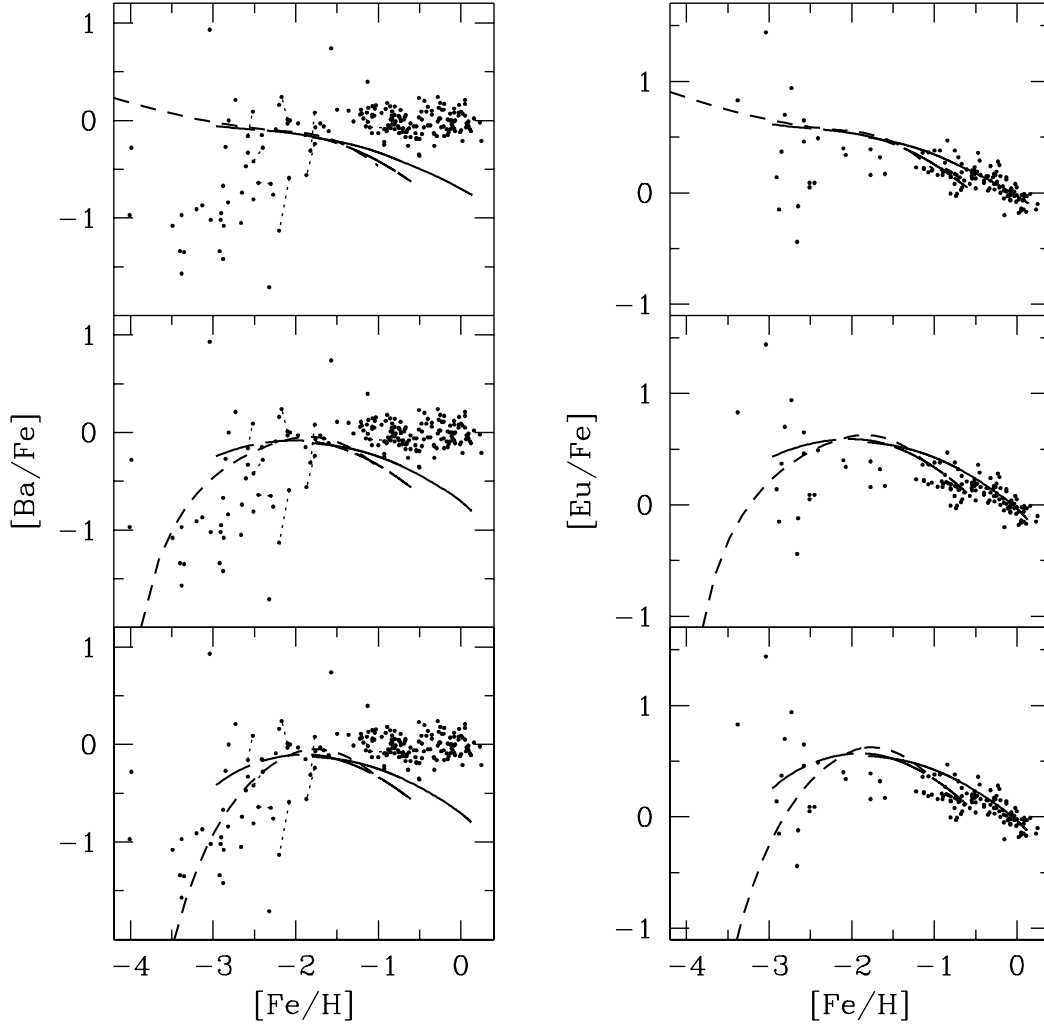


Fig. 5.— Galactic evolution of the r -fraction of Ba (*left panels*) and Eu (*right panels*) according to our standard model, for different assumptions on the mass range of SNII contributing to the r -process nucleosynthesis (all SNII in the upper panels, $10\text{--}12 M_{\odot}$ SNII in the middle panels, $8\text{--}10 M_{\odot}$ SNII in the bottom panels). Lines refer to the halo (*short-dashed*), thick-disk (*long-dashed*) and thin-disk (*solid*). Data points are the same as in Fig. 4 and 12 (errorbars are omitted for clarity).

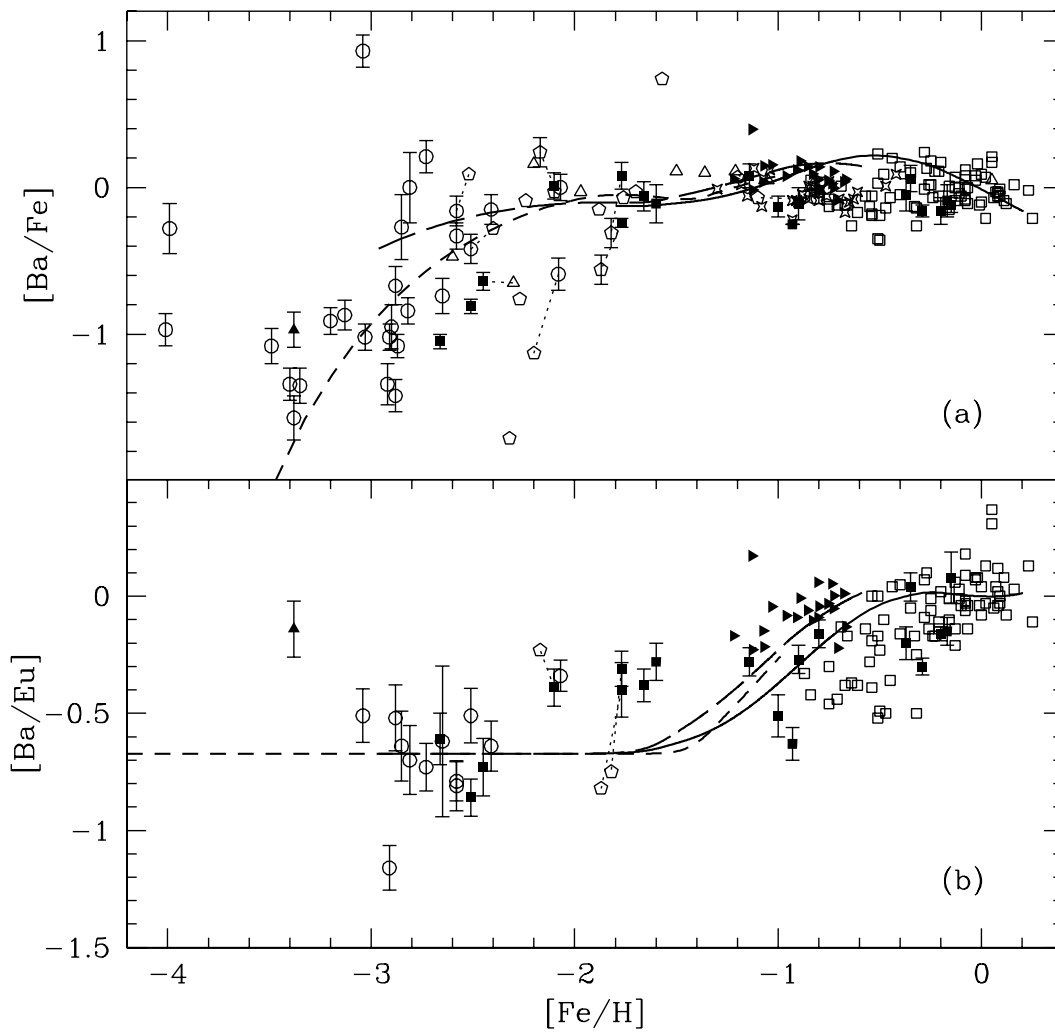


Fig. 6.— Galactic evolution of $[Ba/Fe]$ (*upper panel*) and $[Ba/Eu]$ (*lower panel*) according to our standard model, including both the s - and r -process contributions. All symbols are the same as in in Fig. 4. Errorbars are shown only when reported by the authors for single objects.

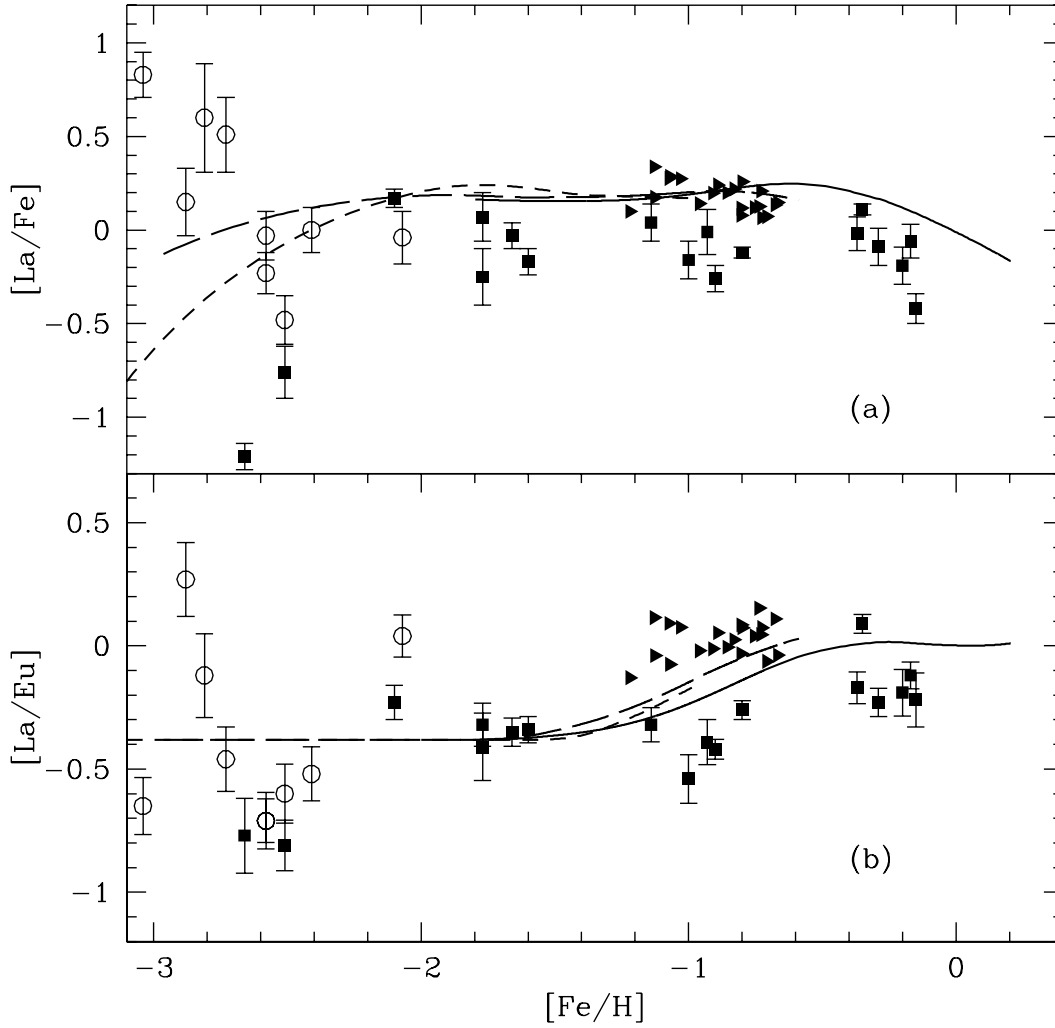


Fig. 7.— Galactic evolution of $[La/Fe]$ (*upper panel*) and $[La/Eu]$ (*lower panel*). All symbols are the same as in in Fig. 4. Errorbars are shown only when reported by the authors for single objects.

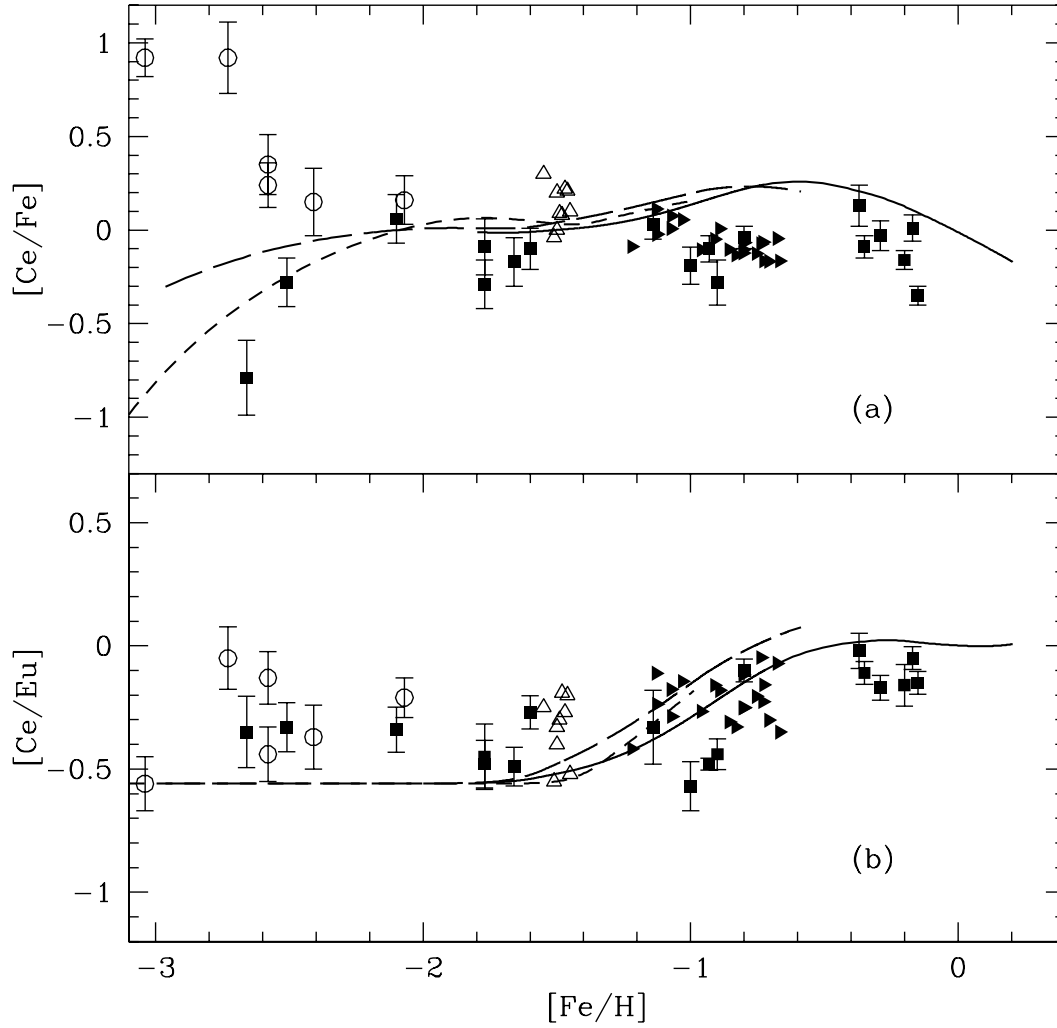


Fig. 8.— Galactic evolution of $[Ce/Fe]$ (*upper panel*) and $[Ce/Eu]$ (*lower panel*). All symbols are the same as in in Fig. 4. Errorbars are shown only when reported by the authors for single objects.

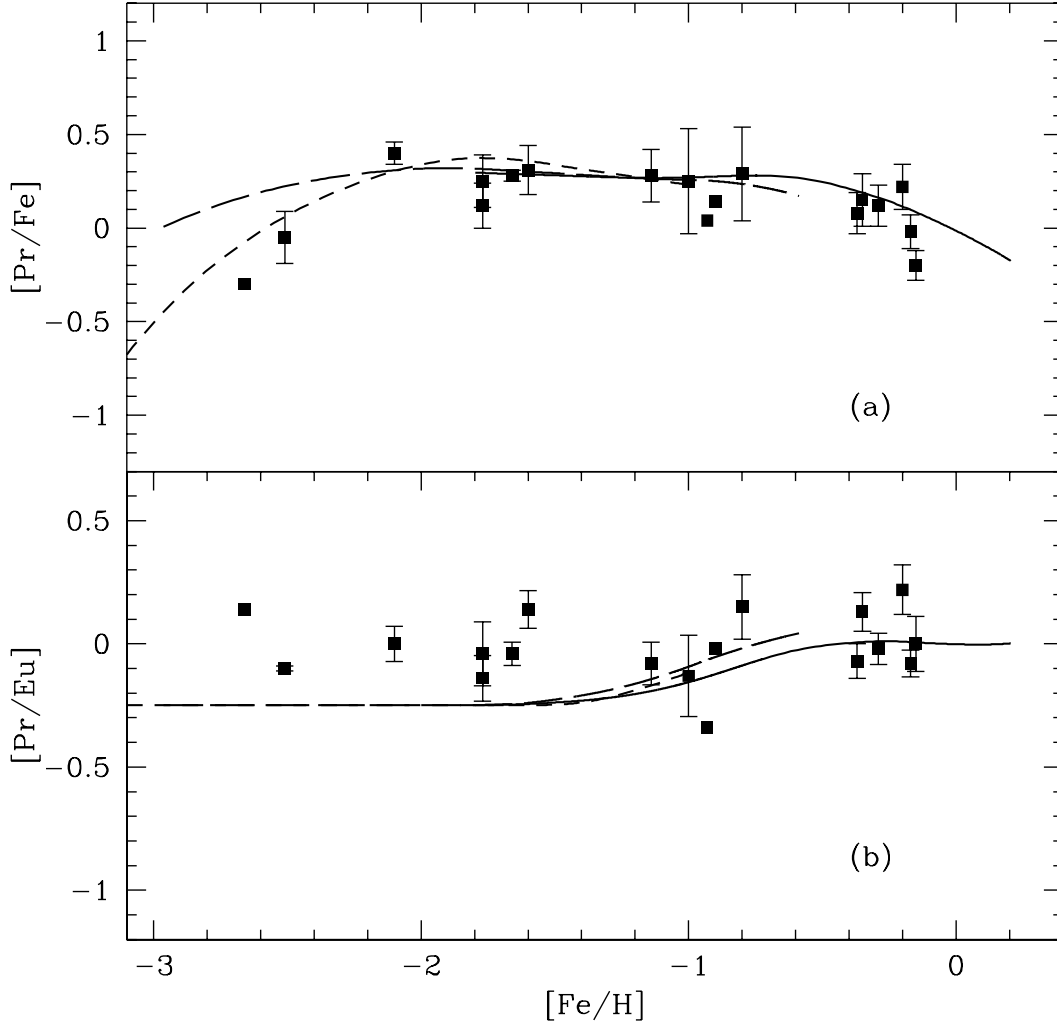


Fig. 9.— Galactic evolution of $[Pr/Fe]$ (*upper panel*) and $[Pr/Eu]$ (*lower panel*). All symbols are the same as in in Fig. 4. Errorbars are shown only when reported by the authors for single objects.

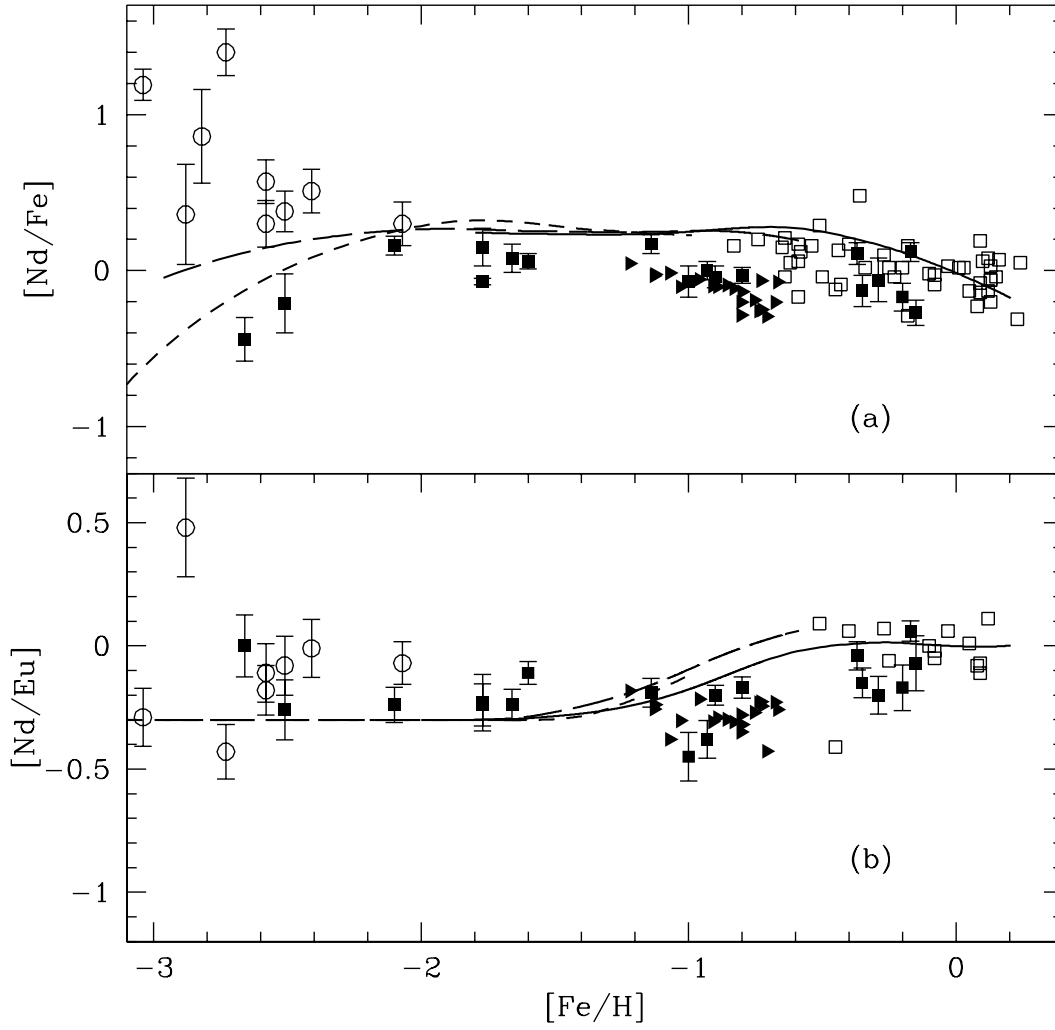


Fig. 10.— Galactic evolution of $[\text{Nd}/\text{Fe}]$ (*upper panel*) and $[\text{Nd}/\text{Eu}]$ (*lower panel*). All symbols are the same as in in Fig. 4. Errorbars are shown only when reported by the authors for single objects.

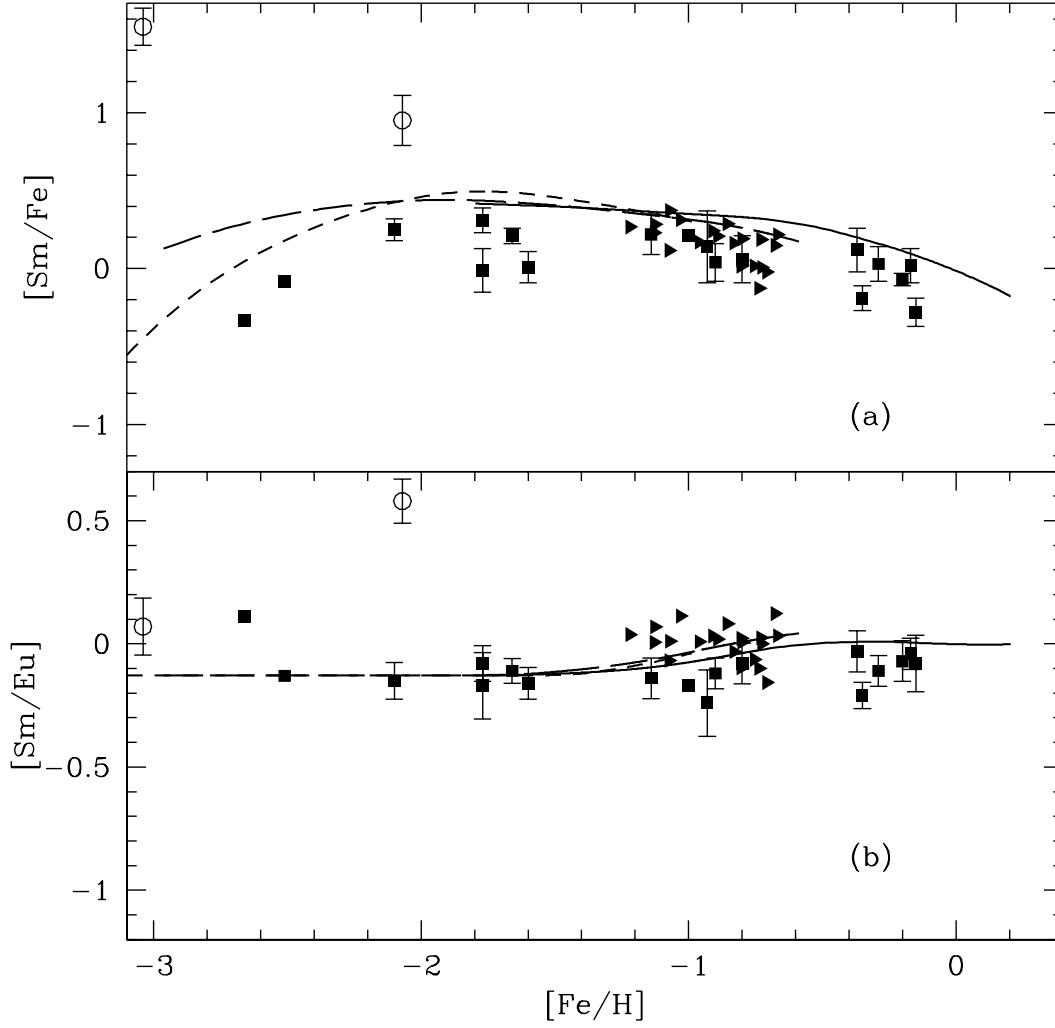


Fig. 11.— Galactic evolution of $[Sm/Fe]$ (*upper panel*) and $[Sm/Eu]$ (*lower panel*). All symbols are the same as in in Fig. 4. Errorbars are shown only when reported by the authors for single objects.

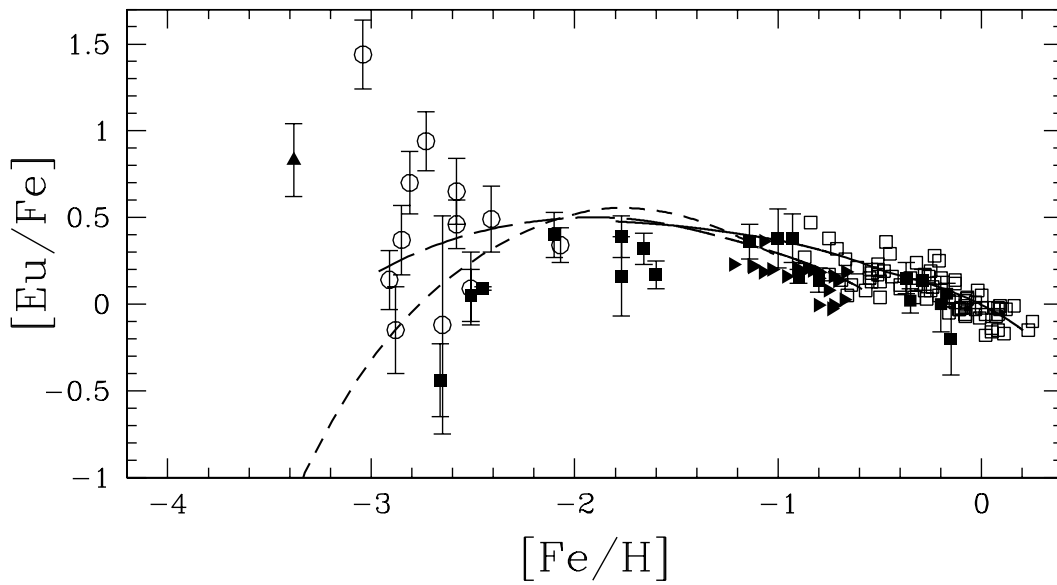


Fig. 12.— Galactic evolution of $[\text{Eu}/\text{Fe}]$ according to our standard model, including both the s - and r -process contributions (even at $t = t_{\text{Gal}}$ the latter component accounts for 94% of the total production). All symbols are the same as in in Fig. 4. Errorbars are shown only when reported by the authors for single objects.

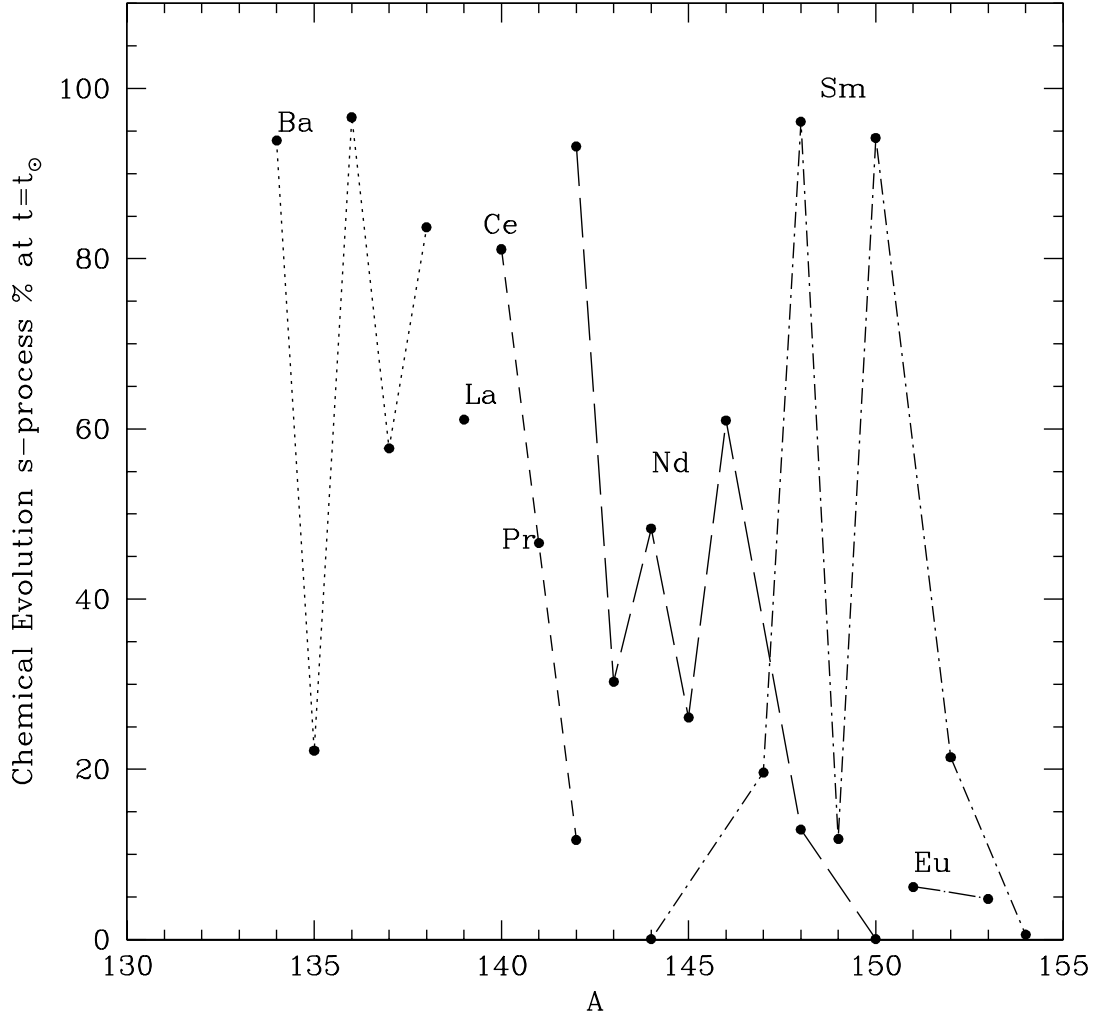


Fig. 13.— s -fractions at $t = t_{\odot}$ of Ba to Eu isotopes, according to our standard model. Values are given in percentage with respect to solar abundances.